УДК 532.526.4

ТЕОРИЯ ТУРБУЛЕНТНОСТИ И МОДЕЛЬ ВЛИЯНИЯ ПЛОТНОСТИ ШЕРОХОВАТОСТИ

Трунев Александр Петрович
к. ф.-м. н., Ph.D., директор
A&E Trounev IT Consulting, Торонто, Канада

В работе представлена модель турбулентного пограничного слоя над шероховатой поверхностью. Модель основана на специальном преобразовании уравнения Навье-Стокса. Турбулентный пограничный слой в этой модели рассматривается как течение над шероховатой поверхностью, генерируемой вязким подслоем (эффект динамической шероховатости). Дана оценка влияния шероховатой стенки на параметры логарифмического профиля в случае 2D и 3D элементов шероховатости

Ключевые слова: ТУРБУЛЕНТНЫЙ ПОГРАНИЧНЫЙ СЛОЙ, ЛОГАРИФМИЧЕСКИЙ ПРОФИЛЬ, ПЛОТНОСТЬ ШЕРОХОВАТОСТИ

UDC 532.526.4

TURBULENCE THEORY AND ROUGHNESS DENSITY EFFECT MODEL

Alexander Trunev
Ph.D., Director
A&E Trounev IT Consulting, Toronto, Canada

The model of the turbulent boundary layer over a rough surface is presented. The model is based on the special type of transformation of the Navier-Stokes equation. The turbulent boundary layer in this model is considered as a flow above the rough surface generated by the viscous sublayer (the dynamic roughness effect). The roughness density effect on the shift of the mean velocity logarithmic profile has been estimated in the case of 2D and 3D roughness elements

Keywords: TURBULENT BOUNDARY LAYER, LOGARITHMIC PROFILE, ROUGHNESS DENSITY EFFECT

1. Introduction

The study of the rough wall turbulence is important in fluid mechanics, in the atmosphere and ocean and in engineering flows. The rough surface effect on the turbulent boundary layer has been considered by Nikuradse (1933) Schlichting (1936, 1960), Bettermann (1966), Dvorak (1969), Simpson (1973), Dirling (1973), Dalle Donne & Meyer (1977), Jackson (1981), Osaka & Mochizuki (1989), Raupach (1992) and other.

Nikuradse (1933) established (for sand-roughened pipes), that if the roughness height significantly exceeds the viscous sublayer thickness, then the mean velocity profile can be described by the logarithmic function:

$$\frac{U}{u_t} = \frac{1}{k}\ln\frac{z}{k_s} + c_s \qquad (1)$$

where u_t is the friction velocity, $u_t = \sqrt{t / r}$, t is the wall shear stress, r is the fluid density, z is the distance from the wall - see Figure 1, k_s is the characteristic scale of the sand roughness, k, c_s are empirical values. Nikuradse found that $k = 0.4, c_s = 8.5$ for the completely rough regime. He compared the mean velocity profile (1) with the law of the wall, derived by him before in 1932 for turbulent flows in smooth pipes, as follows

$$\frac{U}{u_t} = \frac{1}{k}\ln\frac{u_t z}{n} + c_0 - \frac{\Delta U}{u_t} \qquad (2)$$

where n is the kinematic viscosity, $k = 0.4, c_0 = 5.5$ are the logarithmic profile constants for the hydraulically smooth surface. ΔU is the shift of the mean ve-

locity logarithmic profile which can be defined for the turbulent boundary layer over a rough surface as

$$\frac{\Delta U}{u_t} = \frac{1}{k}\ln\frac{u_t k_s}{n} + D_s \qquad (3)$$

where $D_s \approx -3.0$ for the completely rough regime. Nikuradse has shown that the dimensionless roughness height parameter $k_s^+ = u_t k_s / n$ can be used as an indicator of the rough wall turbulence regime. He proposed to consider three typical cases:

- the hydraulically smooth wall for $0 < k_s^+ \le 5$, $\Delta U = 0$;
- the transitionally rough regime for $5 < k_s^+ < 70$, D_s varies with k_s^+;
- the completely rough regime for $k_s^+ \ge 70$, $D_s \approx -3.0$.

Thus, the sand-roughened wall turbulence depends on the dimensionless roughness height (roughness Reynolds number) k_s^+ as has been established by Nikuradse.

Schlichting (1936), used the Nikuradze's date base and his own experimental results obtained in the water tunnel of rectangular cross section with the upper rough wall, proposed the new form of the equation (1) which is well counted the roughness effect on the turbulent boundary layer by means of the effective wall location (Δz) and the equivalent sand roughness parameter k_{es}. With this parameters the mean velocity profile in the turbulent flow over an arbitrary rough surface can be written in the Nikuradze's form (1) as follows:

$$\frac{U}{u_t} = \frac{1}{k}\ln\frac{z_1}{k_{es}} + c_s \qquad (4)$$

where $z_1 = z - \Delta z$ (see Figure 1). The effective wall location was defined by Schlichting as the mean height of the roughness elements (the location of a "smooth wall that replaces the rough wall in such a manner as to keep the fluid volume the same"). The value k_{es} has been measured by Schlichting for several types of the roughness elements with various shapes, sizes and spacing. The Schlichting's experiment was re-evaluated by Coleman *et. al.* (1984) and they noticed that some Schlichting's data have been obtained in the transitional rough regime.

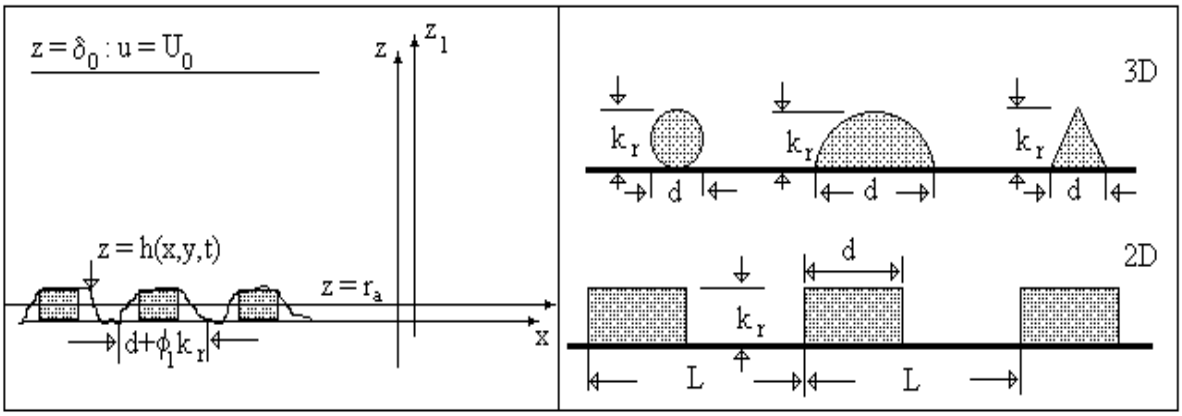

Figure 1: The scheme of the turbulent flow over a rough surface (left), and the roughness elements are considered in the paper (right): spheres, spherical segments, conical elements (3D) and transverse rectangular roods (2D)

Clauser (1956) has shown that the shift of the mean velocity profile can be written as

$$\frac{\Delta U}{u_t} = \frac{1}{k}\ln\frac{u_t k_r}{n} + D$$

where k_r is the characteristic scale of roughness elements and D must be some function of the roughness geometrical parameters. Hence the equivalent sand roughness parameter $k_{es} = k_r \exp[k\,(D - D_s)]$, where $D_s \approx -3.0$ for sand roughness.

Bettermann (1966) discovered that D is the function of the roughness elements spacing. He introduced the roughness density parameter for roughness composed of the transverse square bars as the pith-to-height ratio, $\Lambda_B = L / k_r$ - see Figure 1. Bettermann found that in the range $1 \le \Lambda_B \le 5$ the variations of D with the roughness density can be specified by

$$D = 12.25\ln\Lambda_B - 17.35$$

As has been demonstrated by Dvorak (1969), the rough wall effect is well correlated with the roughness density parameter defined as pitch-to-width ratio or the ratio of total surface area to roughness area, $\Lambda_s = L / d$. Dvorak developed the Bettermann's model in the range $4.68 \le \Lambda_s \le 10^2$, used the data of Schlichting and other researches, as follows:

$$D = \begin{cases} 12.25\ln\Lambda_s - 17.35, & 1 \le \Lambda_s \le 4.68 \\ -2.85\ln\Lambda_s + 5.95, & \Lambda_s > 4.68 \end{cases} \qquad (5)$$

Simpson (1973) introduced the roughness density parameter in the case of three-dimensional (3D) roughness as $\Lambda^*_S = (N_S A_F)^{-1}$, where N_S is the number of significant roughness elements per unit area, A_F is the average frontal area of the "significant" roughness elements. He suggested the general interpretation of the

Bettermann-Dvorak correlation (5): two branches (5) exist depending on the formation or absence of transverse vortices between roughness elements. Simpson also showed that the shape of the element is an important parameter.

The model been reported by Dirling (1973) and verified by Grabow & White (1975), takes into consideration the roughness elements shape parameters. The Dirling's density parameter is defined as $\Lambda_D = (L / k_r)(A_W / A_F)^{4/3}$ where A_W is "the windward wetted surface area". In a case of two-dimensional (2D) roughness the Dirling's parameter leads to the Bettermann's roughness density parameter. As it was shown by Sigal & Danberg (1990) the shape parameters effect can be described by the similar correlation such equation (5) and that $D = 2.2$ for the two-dimensional roughness in the range $4.89 \le \Lambda_s \le 13.25$. They also underlined that the correlation for 2D roughness elements is not the same as for 3D elements. On the other hand, Kind & Lawrysyn (1992) confirmed that the Bettermann-Dvorak function $D(\Lambda_s)$ in the form (5) can be successfully used for the correlation of the experimental data in the aerodynamic experiments with the natural hoar-frost roughness.

Dalle Donne & Meyer (1977) correlated their data and those of previous researches (19 data bases considered below in section 3.4) used the roughness density parameter $\Lambda_D^* = (L - d) / k_r$. They developed the empirical model which can be applied to the turbulent flows in the annuli and tubes with inner surface roughened by rectangular ribs.

Osaka & Mochizuki (1989) examined d-type rough wall boundary layer in a transitional and a fully rough regime. They have shown that in a transitional rough regime the mean velocity logarithmic profile is confirmed and that the Karman constant has the same value as for the hydraulically smooth wall flow.

The mean velocity logarithmic profile widely used in the atmospheric turbulence research is given by (see Monin & Yaglom (1965)):

$$\frac{U}{u_t} = \frac{1}{k} \ln \frac{z - z_d}{z_0}$$

where z_d is the displacement height, z_0 is the roughness length. Note that z_d and z_0 are considered often as some adjustment parameters chosen for the best correlation of the local wind profile in the neutral stratified flow with the logarithmic profile. The model of the displacement height has been considered by Jackson (1981). The roughness length model was developed by Raupach (1992) and other. The classification of the experimentally determined roughness length for various terrain types was given by Wieringa (1992).

The objective of the present work is to develop the model of the turbulent boundary layer which can be applied to any cases considered above: turbulent flows over smooth surfaces, in the transitional rough regime and for the fully developed roughness. The main idea is to derive the model of the turbulent flow

over a rough surface directly from the Navier-Stokes equation. As shown in section 2 the requisite model can be derived from the transformed and averaged Navier-Stokes equation due to the *surface layer transformation* introduced by Trunev & Fomin (1985) in the impingement erosion model and developed by Trunev (1995, 1996, 1997, 1999, 2000) for the turbulent boundary layer problem.

2. Turbulent flow model

2.1. Surface layer transformation

The effective wall location was defined by Schlichting (1936) as the mean height of the roughness elements and in the mathematical form can be written as:

$$\Delta z = r_a = \frac{1}{L_x L_y} \iint_{\Delta x \Delta y} r(x,y)dxdy \qquad (6)$$

where $z = r(x,y)$ is the relief of the rough surface - see Figure 1, L_x, L_y are the rough wall scales in the x, y directions, $\Delta x \Delta y = L_x L_y$. In a case of two dimensional roughness considered by Dvorak (1969) and Simpson (1973) the roughness density parameter depends on width and pitch of the roughness elements (see Figure 1): $\Lambda_s = L/d$. The mean roughness height depends on the height of roughness elements as $r_a = ak_r / \Lambda_s$, where a is the numerical constant which equals to unity in this case. The shift of the mean velocity can be presented as a function of the mean roughness height. Thus using the Bettermann-Dvorak's equation (5) in the range $4.68 \le \Lambda_s \le 10^2$, we have

$$\frac{\Delta U}{u_t} = \frac{1}{k}\ln\frac{u_t k_r}{n} + D \approx 2.5\ln\frac{u_t k_r}{n\,\Lambda_s} - 0.35\ln\Lambda_s + 5.95 = 2.5\ln\frac{u_t r_a}{n} - 0.35\ln\Lambda_s + 5.95$$

In this approach the mean velocity profile in the turbulent flow over a rough surface can be rewritten as follows

$$\frac{U}{u_t} = \frac{1}{k}\ln\frac{z_1}{r_a} + 0.35\ln\Lambda_s - 0.45$$

If we redefined the main roughness scale then the mean velocity profile takes the form which is widely used in the atmosphere research:

$$\frac{U}{u_t} = \frac{1}{k}\ln\frac{z_1}{r_0} \qquad (7)$$

where $\ln r_0 = \ln r_a - 0.35k\ln\Lambda_s + 0.45k \approx \ln r_a - 0.14\ln\Lambda_s + 0.18$. Practically $r_0 \approx r_a$ for $\Lambda_s = 5$ and $r_0 \approx 0.63 r_a$ for $\Lambda_s = 100$. Hence, the logarithmic profile mainly depends on the mean height of the roughness elements in this range of the roughness density.

Let us consider the random function defined as

$$\tilde{u}(z_1 / r) = \frac{u_t}{k} \ln \frac{z_1}{r} \tag{8}$$

where r is the random parameter with the mean value given by

$$r_a = \int_0^\infty r f_s(r) dr$$

here $f_s = f_s(r)$ is the density of a probability distribution function (roughness statistic function) normalised on unity:

$$\int_0^\infty f_s(r) dr = 1$$

Both parts of the equation (8) can be averaged with this function as follows:

$$U(z_1) = \int_0^\infty \tilde{u}(z_1 / r) f_s(r) dr = \frac{u_t}{k} \int_0^\infty \left(\ln z_1 - \ln r \right) f_s(r) dr = \frac{u_t}{k} \ln \frac{z_1}{r_0}$$

where $\ln r_0 = \int_0^\infty \ln(r) f_s(r) dr$. With this result the mean-squared-value of the velocity fluctuations can be calculated as

$$dU^2 = \int_0^\infty (\tilde{u} - U)^2 f_s(r) dr = \frac{u_t}{k} \int_0^\infty \left(\ln r - \ln r_0 \right)^2 f_s(r) dr = \frac{u_t}{k} \left(\left\langle \ln^2 r \right\rangle - \ln^2 r_0 \right)$$

Thus, the random function $\tilde{u}(z_1 / r)$ can be used for the mean velocity calculation as well as for the mean-squared-value of the velocity fluctuations modelling. Our main idea is that the random function $\tilde{u}(z_1 / r)$ can be calculated on the basis of a solution of the Navier-Stokes equation due to the *surface layer transformation*

$$\tilde{u}(z_1 / r) = \lim_{dV \to dV_s} \frac{1}{dV} \int_{dV} u(x, y, h_1) dx dy dz \tag{9}$$

where $h_1 = z_1 / r(x, y)$ is fixed over the integrated region, $h_1 = z_1 / r = const$, dV is an arbitrary volume put in $dV = L_x L_y dz$ and containing dV_s as a whole, dV_s is the subregion in which altitude of the rough surface $r(x, y)$ varies in limits from r up to $r + dr$, hence by definition $dV_s = dV f_s(r) dr$.

Note, that the surface layer transformation is only a kind of averaging procedure which conserves the function properties across a boundary layer. The Navier-Stokes equation can be averaged with the surface layer transformation (9) instead of normal Reynolds averaging method to derive then the equation for the random function $\tilde{u}(z_1 / r)$. Unfortunately it's impossible to use this method in the simple form (9), because, for example, in the case of a smooth flat plate $r = 0$.

Therefore we suppose that there is a surface $z = h(x, y, t)$ (the dynamic roughness surface) inside the flow domain which can be used for modelling the rough sur-

face effect on the turbulent boundary layer. Without any limits we can choose a surface $z = h(x,y,t)$ close to the wall surface $z = r(x,y)$, but not equal to $r(x,y)$. Let $h(x,y,t) = r(x,y) + h_r(x,y,t)$, where $h_r(x,y,t)$ is the height of the viscous sublayer over the rough surface. In the turbulent flow the surface $z = h(x,y,t)$ can be described by random continuous parameters h, h_t, h_x, h_y characterising the height, velocity and inclination of the surface elements. Let's define the subregion dV_s in which the local height of the rough surface $r(x,y)$ varies in limits from r up to $r + dr$ and parameters of the surface $z = h(x,y,t)$ in limits from h up to $h + dh$, from h_t up to $h_t + dh_t$, from h_x up to $h_x + dh_x$, from h_y up to $h_y + dh_y$, thus $dV_s = dVf_s(r,h,h_x,h_y,h_t)drdhdh_xdh_ydh_t$, where $f_s = f_s(r,h,h_x,h_y,h_t)$ is the multiple density of a probability distribution function. Thus in common case the surface layer transformation can be written as follows (instead of eq. (9))

$$\tilde{\mathbf{u}}(z_1 / h,t,r,h,h_x,h_y,h_t) = \lim_{dV \to dV_s} \frac{1}{dV} \int_{dV} \mathbf{u}(x,y,h,t)dxdydz \qquad (10)$$

where $h = z_1 / h(x,y,t)$ is fixed over the region of integration, $h = z_1 / h = const$, dV is an arbitrary volume put in $dV = L_x L_y dz$ and containing dV_s as a whole. Statistical moment of order m of a random function $\tilde{\mathbf{u}}(z_1 / h,t,r,h_t,h_x,h_y)$ is given by

$$\overline{\tilde{u}_i}^m(z_1,t) = \int \tilde{u}_i^m(h_1,t,r,h,h_x,h_y,h_t) f_s(r,h,h_x,h_y,h_t)drdhdh_xdh_ydh_t \qquad (11)$$

The main problem of this method is how to estimate the multiple density of a probability distribution function $f_s = f_s(r,h,h_x,h_y,h_t)$? Nevertheless, for the solutions presented by the logarithmic function we can suppose that

$$\overline{\tilde{u}} = \int \tilde{u}(h_1,t,r,h,h_x,h_y,h_t) f_s(r,h,h_x,h_y,h_t)drdhdh_xdh_ydh_t = \tilde{u}(z_1 / h_*, r_*, h_x^*, h_y^*, h_t^*)$$

where the parameters with stars can be estimated from the comparison of solutions with experimental data or calculated from some theoretical considerations. Practically the roughness parameter r_* should be given as an input value and all another parameters can be calculated from the similarity theory considered in sections 2.6-2.7.

2.2. Input equations

We shall consider the turbulent flow of fluid containing a scalar impurity. Fluid is assumed as viscous, heat-conducting, incompressible gas in a rather slow turbulent motion. Thus, the model of the turbulent flow is given by:

$$\nabla.\mathbf{u} = 0 \qquad (12)$$

$$\frac{\partial \mathbf{u}}{\partial t} + (\mathbf{u}.\nabla)\mathbf{u} + \frac{\nabla p}{r_0} = n\nabla^2\mathbf{u}$$

$$\frac{\P T}{\P t}+(\mathbf{u}.\nabla)T=\frac{n}{\mathbf{Pr}}\nabla^2 T, \qquad \frac{\P C}{\P t}+(\mathbf{u}.\nabla)C=\frac{n}{\mathbf{Sc}}\nabla^2 C$$

where r is the fluid density, $\mathbf{u}=(u,\mathrm{v},w)$ is the flow velocity vector, n is the kinematics viscosity, p is the pressure, T is the temperature, Pr is the Prandtl number, C is the mass concentration of an impurity, $\mathrm{Sc}=n/D$ is the Schmidt number, D is the molecular diffusion coefficient.

Boundary conditions for the flow parameters are set as follows:

$$z=r(x,y):\ \mathrm{u}=0,\quad T=T_g,\quad C=C_g \tag{13}$$

$$z=d_0:\mathbf{u}=(U_0,0,0),T=T_0,C=C_0$$

where T_g is the surface temperature, C_g is the impurity concentration at the wall, d_0 is the boundary layer thickness, U_0,T_0,C_0 are the flow velocity the temperature and the impurity concentration in the distance $z=d_0$ respectively.

2.3. Random flow parameters equations

The nontrivial solutions of the Navier-Stokes equations which may play important role in the surface layer turbulent flow organisation can be written as $\mathbf{u}=\mathbf{u}(x,y,z/h(x,y,t),t)$, where $z=h(x,y,t)$ is the dynamic roughness surface. Due to the special type of transformation in the form (10) the velocity field, the pressure, the temperature and concentration are transformed as

$$\mathbf{S}=(\mathbf{u},p,T,C)\longrightarrow\tilde{\mathbf{S}}=(\tilde{\mathbf{u}},\tilde{p},\tilde{T},\tilde{C})$$

The equations for the random functions $\tilde{\mathbf{S}}(z/h,t,r,h,h_t,h_x,h_y)$ can be derived from the equations (12) written in the curvilinear coordinate system (x,y,h,t). Following Pulliam & Steger (1980) the equations (12) are presented in the form:

$$\frac{\P\mathbf{Q}}{\P t}+\frac{\P}{\P x}(\mathbf{E}-\mathbf{E}_v)+\frac{\P}{\P y}(\mathbf{F}-\mathbf{F}_v)+J\frac{\P}{\P h}(\mathbf{G}-\mathbf{G}_v)+$$

$$+J\left[h_t\mathbf{Q}+h_x(\mathbf{E}-\mathbf{E}_v)+h_y(\mathbf{F}-\mathbf{F}_v)\right]=0 \tag{14}$$

where J is the Jacobian, $J=h^{-1}\neq 0,\ J^{-1}=h\neq 0$,

$$\mathbf{Q}=\begin{pmatrix} r\\ ru\\ rv\\ rw\\ T\\ C\end{pmatrix},\mathbf{E}=\begin{pmatrix} ru\\ ru^2+p\\ ruv\\ ruw\\ uT\\ uC\end{pmatrix},\mathbf{F}=\begin{pmatrix} rv\\ ruv\\ rv^2+p\\ rwv\\ vT\\ vC\end{pmatrix},\mathbf{G}=\begin{pmatrix} rW\\ ruW-hh_xp\\ rvW-hh_yp\\ rwW+p\\ WT\\ WC\end{pmatrix},$$

$$\mathbf{E}_v = \begin{pmatrix} 0 \\ t_{xx} \\ t_{yx} \\ t_{zx} \\ n\,\mathbf{Pr}^{-1}T_x \\ DC_x \end{pmatrix}, \mathbf{F}_v = \begin{pmatrix} 0 \\ t_{xy} \\ t_{yy} \\ t_{zy} \\ n\,\mathbf{Pr}^{-1}T_y \\ DC_y \end{pmatrix}, \mathbf{G}_v = \sum_i \begin{pmatrix} \mathbf{0} \\ h_i t_{xi} \\ h_i t_{yi} \\ h_i t_{zi} \\ n\,\mathbf{Pr}^{-1}h_i T_i \\ Dh_i C_i \end{pmatrix}$$

Here t_{kl} is the tensor of viscous stress, $t_{kl} = m\left(\frac{\partial u_l}{\partial x_k} + \frac{\partial u_k}{\partial x_l}\right)$, m is the dynamic viscosity, $k,l = 1,2,3$; $h_x = -Jh\,h_x, h_y = -Jh\,h_y, h_z = J, W = w - h(h_t + h_x u + h_y \mathrm{v}), i = x, y, z$

In curvilinear coordinate system it is necessary to execute replacements in terms with gradients:

$$\frac{\partial}{\partial x_j} \to \frac{\partial}{\partial x_j} + \frac{\partial h}{\partial x_j}\frac{\partial}{\partial h} \quad \text{for } j = 1,2; \quad \frac{\partial}{\partial z} \to \frac{1}{h}\frac{\partial}{\partial h},$$

Let us consider the special types of solution of transformed equations (14) which depend only on time and normal variable h as it often suggested in the turbulent boundary layer theory. Thus let's suppose that $\frac{\partial}{\partial x}(\mathbf{E} - \mathbf{E}_v) = \frac{\partial}{\partial y}(\mathbf{F} - \mathbf{F}_v) = 0$ in the left part of (14). In this case eq. (14) can be presented in the form

$$\frac{\partial \tilde{\mathbf{Q}}}{\partial t} + \frac{1}{h}\frac{\partial}{\partial h}(\tilde{\mathbf{G}} - \tilde{\mathbf{G}}_v) + J\left[h_t \tilde{\mathbf{Q}} + h_x(\tilde{\mathbf{E}} - \tilde{\mathbf{E}}_v) + h_y(\tilde{\mathbf{F}} - \tilde{\mathbf{F}}_v)\right] = 0 \qquad (14')$$

where parameters with tilde are defined similar to $\tilde{\mathbf{S}} = (\tilde{\mathbf{u}}, \tilde{p}, \tilde{T}, \tilde{C})$ as it follows from (10). In the equation (14') the dissipate terms can be written as

$$\tilde{\mathbf{E}}_v = -\frac{h}{h}\begin{pmatrix} 0 \\ 2mh_x\tilde{u}_h \\ mh_y\tilde{u}_h + mh_x\tilde{\mathrm{v}}_h \\ mh_x\tilde{w}_h - m\tilde{u}_h/h \\ n\,\mathbf{Pr}^{-1}h_x\tilde{T}_h \\ Dh_x\tilde{C}_h \end{pmatrix}, \quad \tilde{\mathbf{F}}_v = -\frac{h}{h}\begin{pmatrix} 0 \\ mh_x\tilde{\mathrm{v}}_h + mh_y\tilde{u}_h \\ 2mh_y\tilde{\mathrm{v}}_h \\ mh_y\tilde{w}_h - m\tilde{\mathrm{v}}_h/h \\ n\,\mathbf{Pr}^{-1}h_y\tilde{T}_h \\ Dh_y\tilde{C}_h \end{pmatrix}, \quad \tilde{\mathbf{G}}_v = (1+n^2h^2)\frac{1}{h}\frac{\partial}{\partial h}\begin{pmatrix} 0 \\ m\tilde{u} \\ m\tilde{\mathrm{v}} \\ m\tilde{w} \\ n\,\mathbf{Pr}^{-1}\tilde{T} \\ D\tilde{C} \end{pmatrix}$$

where $\tilde{u}_h = \partial\tilde{u}/\partial h$, ….

On the other hand to derive the equation (14') one can applied the averaging operator in the form (10) with an arbitrary averaging volume dV to equation (14)

to conserve the commutative properties of the averaging operator with the space and time differential operators. Then one can consider the limit of all terms of the averaged equation at $dV \to dV_s$. At this step the theorem about two limits of the continuous function can be used (since the differential operators can be considered as some limits). Note, if $\tilde{\mathbf{S}} = (\tilde{\mathbf{u}}, \tilde{p}, \tilde{T}, \tilde{C})$ is the solution of the transformed Navier-Stokes equations (14) in any sense, then we have the turbulence model closures automatically as follows:

$$\lim_{dV \to dV_s} \frac{1}{dV} \int_{dV} u_i(x,y,h,t) u_k(x,y,h,t) dxdydz = \tilde{u}_i \tilde{u}_k + q d_{ik}$$

$$\lim_{dV \to dV_s} \frac{1}{dV} \int_{dV} \mathbf{u}(x,y,h,t) T(x,y,h,t) dxdydz = \tilde{\mathbf{u}} \tilde{T}$$

$$\lim_{dV \to dV_s} \frac{1}{dV} \int_{dV} \mathbf{u}(x,y,h,t) C(x,y,h,t) dxdydz = \tilde{\mathbf{u}} \tilde{C}$$

Here $3q/2$ is the kinetic energy of turbulent fluctuations in the small volume dV_s, d_{ik} is the Kronecker delta: $d_{ik} = 0$ for $i \neq k$, $d_{ik} = 1$ for $i = k$.

Note, that in this model the Reynolds stress can be calculated as

$$t'_{ik}(z,t) = \int r[(\tilde{u}_i - \overline{\tilde{u}}_i)(\tilde{u}_k - \overline{\tilde{u}}_k) + q d_{ik}] f_s(r,h,h_x,h_y,h_t) dr dh dh_x dh_y dh_t$$

Therefore the random function $\tilde{\mathbf{u}} = \tilde{\mathbf{u}}(h,t,r,...)$ gives the main contribution in the non-diagonal components of the Reynolds stress. Now we take it as granted because we haven't any contradictions. Hence, the first assumption of this theory is that the turbulence interaction between the hydrodynamic fields can be described with the solutions $\tilde{\mathbf{S}} = (\tilde{\mathbf{u}}, \tilde{p}, \tilde{T}, \tilde{C})$ as well as with the solutions $\mathbf{S} = (\mathbf{u}, p, T, C)$. The second assumption is that it's possible to neglect longitudinal and transversal gradients of flow parameters in a comparison with gradients across a boundary layer, at least for steady turbulent flow. Finally we have the dynamic equations for random flow parameters as follows:

$$\frac{\partial \tilde{w}}{\partial h} - h \frac{\partial \Phi}{\partial h} = 0 \qquad (15)$$

$$\frac{\partial \tilde{\mathbf{u}}}{\partial t} + \frac{\tilde{W}}{h} \frac{\partial \tilde{\mathbf{u}}}{\partial h} + \frac{\mathbf{N}}{rh} \frac{\partial \tilde{P}}{\partial h} = \frac{n}{h^2} \frac{\partial}{\partial h} (1 + n^2 h^2) \frac{\partial \tilde{\mathbf{u}}}{\partial h} - \frac{n n^2 h}{h^2} \frac{\partial \tilde{\mathbf{u}}}{\partial h} + \frac{n \mathbf{N}}{h^2} \frac{\partial \Phi}{\partial h}$$

$$\frac{\partial \tilde{T}}{\partial t} + \frac{\tilde{W}}{h} \frac{\partial \tilde{T}}{\partial h} = \frac{n}{\mathrm{Pr} h^2} \frac{\partial}{\partial h} (1 + n^2 h^2) \frac{\partial \tilde{T}}{\partial h} - \frac{n n^2 h}{\mathrm{Pr} h^2} \frac{\partial \tilde{T}}{\partial h}$$

$$\frac{\partial \tilde{C}}{\partial t} + \frac{\tilde{W}}{h} \frac{\partial \tilde{C}}{\partial h} = \frac{n}{\mathrm{Sc} h^2} \frac{\partial}{\partial h} (1 + n^2 h^2) \frac{\partial \tilde{C}}{\partial h} - \frac{n n^2 h}{\mathrm{Sc} h^2} \frac{\partial \tilde{C}}{\partial h}$$

where $\Phi = h_t + h_x\tilde{u} + h_y\tilde{v}$; $\tilde{P} = \tilde{p} + q$, $n = \sqrt{h_x^2 + h_y^2}$, $\tilde{W} = \tilde{w} - h\Phi$,
$\mathbf{N} = (-h\ h_x, -h\ h_y, 1)$ (thus the value q included in the turbulent pressure).

The first equation (15) is the continuity equation; the second is the momentum equation.

Note, that the parameters of a dynamic roughness in equations (15), are not already the functions of space variables or time. Really, in virtue of transformation (10), the values of these parameters are fixed in intervals from r up to $r + dr$, from h up to $h + dh$, from h_t up to $h_t + dh_t$, from h_x up to $h_x + dh_x$, from h_y up to $h_y + dh_y$. These values, thus, are considered as the random parameters, and the law of their distribution in specific intervals is described by a known function $f_s = f_s(r, h, h_x, h_y, h_t)$.

As we can see from the derived equations (15) there are the factors in the higher derivatives terms, which depend on a distance up to a rigid surface. It should be noted also, that the equation (14) is not in the strong conservation form, as, for example, it is given by Pulliam & Steger [59]. Therefore the numbers of terms in square brackets, breaking conservation of this system are chosen in the left part of equations (14) and (14'). Such allocation of non-divergent terms is stipulated by the purposes of modelling of the eddy viscosity, which, in our opinion, arises in a boundary layer from transformation of a tensor of viscous stresses in a neighbourhood of a dynamic roughness surface. It is obvious in the case of viscous flow over a rigid rough surface and is connected with an adhesion of a viscous flow to a rigid surface of any configuration. In the turbulent flow over a smooth surface the eddy viscosity is simulated by analogy to a more widespread type of turbulent flows, as in a special case, when $r \to 0$. Thus the eddy viscosity is connected (mathematically) with transformation of a tensor of viscous stresses to coordinate mapping which brings rigid surface onto coordinate surface.

For the diffusion equation it is possible to derive the boundary layer model by the simplified way. Let us suppose that in the last equation (12) $C = C(h(x, y, z, t), t)$, then we have

$$\frac{\partial C}{\partial t} + (\mathbf{u}.\nabla)C - \frac{n}{\mathbf{Sc}}\nabla^2 C = \frac{\partial C}{\partial t} + (h_t + \mathbf{u}.\nabla h)\frac{\partial C}{\partial h} - D(\nabla h)^2\frac{\partial^2 C}{\partial h^2} - D\nabla^2 h\frac{\partial C}{\partial h} = 0$$

In partial case when $h = z / h(x, y, t)$ thus

$$\nabla h = h^{-1}(-hh_x, -hh_y, 1); \quad \nabla^2 h = -hh^{-1}\nabla^2 h + 2h(h^{-1}\nabla h)^2,$$

and therefore the last equation can be written as

$$\frac{\P C}{\P t}+\frac{W}{h}\frac{\P C}{\P h}=\frac{D}{h^2}(1+n^2h^2)\frac{\P^2 C}{\P h^2}+\frac{2Dn^2h}{h^2}\frac{\P C}{\P h}-\frac{Dh\nabla^2 h}{h}\frac{\partial C}{\partial h}$$

This equation can be transformed to the form of the last equation (15). According to definition

$$\tilde{C}(h,t,r,h,h_x,h_y,h_t)=\lim_{dV\to dV_s}\frac{1}{dV}\int_{dV}C(h,t)dxdydz,$$

Using the identity $h^{-1}\nabla^2 h=\nabla(h^{-1}\nabla h)+h^{-2}\nabla^2 h$, and averaging all terms, finally we have

$$\frac{\P\tilde{C}}{\P t}+\frac{\tilde{W}}{h}\frac{\P\tilde{C}}{\P h}=\frac{D}{h^2}(1+n^2h^2)\frac{\P^2\tilde{C}}{\P h^2}+\frac{Dn^2h}{h^2}\frac{\P\tilde{C}}{\P h}-$$
$$-\lim_{dV\to dV_s}\frac{1}{dV}\int dzDh\frac{\partial C}{\partial h}\int_{\Delta S}\nabla(h^{-1}\nabla h)dxdy$$

where $\Delta S=L_xL_y$. But the last term is annulled if region $\Delta S=L_xL_y$ is large enough (the divergence theorem). Therefore we have an equation

$$\frac{\P\tilde{C}}{\P t}+\frac{\tilde{W}}{h}\frac{\P\tilde{C}}{\P h}=\frac{D}{h^2}(1+n^2h^2)\frac{\P^2\tilde{C}}{\P h^2}+\frac{Dn^2h}{h^2}\frac{\P\tilde{C}}{\P h}=\frac{n}{\mathrm{Sc}h^2}\frac{\partial}{\partial h}(1+n^2h^2)\frac{\P\tilde{C}}{\P h}-\frac{nn^2h}{\mathrm{Sc}h^2}\frac{\P\tilde{C}}{\P h},$$

which is identical to the last equation (15).

2.4. Pressure integral and random flow parameters equations transformation

In the case of an isothermal incompressible flow the hydrodynamic part of the equations (15) can be written as:

$$\frac{\P\tilde{W}}{\P h}+\Phi=0 \qquad (15')$$

$$\frac{\P\tilde{\mathbf{u}}}{\P t}+\frac{\tilde{W}}{h}\frac{\P\tilde{\mathbf{u}}}{\P h}+\frac{\mathbf{N}}{rh}\frac{\P\tilde{P}}{\P h}=\frac{n}{h^2}\frac{\partial}{\partial h}(1+n^2h^2)\frac{\P\tilde{\mathbf{u}}}{\P h}-\frac{nn^2h}{h^2}\frac{\P\tilde{\mathbf{u}}}{\P h}+\frac{n\mathbf{N}}{h^2}\frac{\P\Phi}{\P h}$$

Put $\mathbf{N_1}=(h_x,h_y,0)$. Multiplying by a scalar way the second equation (15') on the

vectors $\mathbf{N},\mathbf{N_1}$ respectively one can derived the pressure gradient and the equation for the linear combination of momentum components Φ as

$$\frac{\partial \tilde{P}}{\partial h} = \frac{2nr}{h}\frac{\partial \Phi}{\partial h} - \frac{hr}{\mathbf{N}^2}\frac{\partial \tilde{W}}{\partial t} \tag{16}$$

$$\frac{\partial \Phi}{\partial t} + \frac{\tilde{W}}{h}\frac{\partial \Phi}{\partial h} - \frac{n^2 h}{r\,h}\frac{\partial \tilde{P}}{\partial h} = \frac{n}{h^2}\frac{\partial}{\partial h}(1+n^2h^2)\frac{\partial \Phi}{\partial h} - \frac{2n\,n^2 h}{h^2}\frac{\partial \Phi}{\partial h}$$

where $\mathbf{N}^2 = 1+n^2h^2$. Substituting Φ from the continuity equation (15') into the second equation (16) and using the first equation (16) finally we have the closed nonlinear model:

$$\frac{\partial^2 \tilde{W}}{\partial h \partial t} + \frac{\tilde{W}}{h}\frac{\partial^2 \tilde{W}}{\partial h^2} - \frac{n^2 h}{\mathbf{N}^2}\frac{\partial \tilde{W}}{\partial t} = \frac{n}{h^2}\frac{\partial}{\partial h}(1+n^2h^2)\frac{\partial^2 \tilde{W}}{\partial h^2} \tag{17}$$

Multiplying the momentum equation (15') on the vector $\mathbf{N_2} = (h_y, -h_x, 0)$ one can derived the linear equation:

$$\frac{\partial \Psi}{\partial t} + \frac{\tilde{W}}{h}\frac{\partial \Psi}{\partial h} = \frac{n}{h^2}\frac{\partial}{\partial h}(1+n^2h^2)\frac{\partial \Psi}{\partial h} - \frac{n\,n^2 h}{h^2}\frac{\partial \Psi}{\partial h} \tag{18}$$

where $\Psi = h_y\tilde{u} - h_x\tilde{v}$.

Note, that $\tilde{W}$ is the contravariant component of the velocity vector associated with the vertical turbulent movement. As it follows from (17-18), $\tilde{W}$ is the main parameter in this model describing the non-linear turbulent effect.

2.5. Steady turbulent flow model

In the case of a steady turbulent flow put $\frac{\partial \Psi}{\partial t} = \frac{\partial \tilde{W}}{\partial t} = \frac{\partial \Phi}{\partial t} = 0$ in (16-18) then the pressure gradient across boundary layer can be written as

$$\frac{\partial \tilde{P}}{\partial h} = \frac{2nr}{h}\frac{\partial \Phi}{\partial h}$$

Having substituted this expression in the second equation (16) and rewritten (17-18) in the case of a steady turbulent flow one can find

$$\frac{\tilde{W}}{h}\frac{\partial^2 \tilde{W}}{\partial h^2} = \frac{n}{h^2}\frac{\partial}{\partial h}(1+n^2h^2)\frac{\partial^2 \tilde{W}}{\partial h^2} \tag{19}$$

$$\frac{\tilde{W}}{h}\frac{\partial \Phi}{\partial h} = \frac{n}{h^2}\frac{\partial}{\partial h}(1+n^2h^2)\frac{\partial \Phi}{\partial h}$$

$$\frac{\tilde{W}}{h}\frac{\P\Psi}{\P h}=\frac{n}{h^2}\frac{\P}{\P h}(1+n^2h^2)\frac{\P\Psi}{\P h}-\frac{n\,n^2h}{h^2}\frac{\P\Psi}{\P h}$$

The first integrals of the equations (19) are given by

$$\frac{d\Phi}{dh}=\frac{A_1\exp[-I(h)]}{1+n^2h^2},\qquad \frac{d\Psi}{dh}=\frac{A_2\exp[-I(h)]}{\sqrt{1+n^2h^2}},\qquad \frac{d^2\tilde{W}}{dh^2}=-\frac{A_1\exp[-I(h)]}{1+n^2h^2}\quad , \quad (20)$$

where A_i are some constants, $I=-\frac{h}{n}\int_0^h\frac{\tilde{W}\,dh}{1+n^2h^2}$.

Note, that the velocity components are determined as

$$\tilde{u}=n^{-2}\left[(\Phi-h_t)h_x+\Psi h_y\right],\ \tilde{v}=n^{-2}\left[(\Phi-h_t)h_y-\Psi h_x\right],\ \tilde{w}=\tilde{W}+h\,\Phi$$

hence, used (20) one can derive the velocity gradients equations system written in the normal form suitable for the numerical integration:

$$\frac{d\tilde{u}}{dh}=\frac{n^{-2}h_xA_1e^{-I}}{1+n^2h^2}+\frac{n^{-2}h_yA_2e^{-I}}{\sqrt{1+n^2h^2}},\qquad (21)$$

$$\frac{d\tilde{v}}{dh}=\frac{n^{-2}h_yA_1e^{-I}}{1+n^2h^2}-\frac{n^{-2}h_xA_2e^{-I}}{\sqrt{1+n^2h^2}},\qquad \frac{d\tilde{w}}{dh}=\frac{A_1he^{-I}}{1+n^2h^2}$$

2.6. Nonlinear model numerical solution

The first equation (19) has been numerically solved in the case of the turbulent steady flow over a smooth surface with boundary conditions at

$$h=0:\quad \tilde{W}(0)=0,\quad d\tilde{W}/dh=-h_t,\quad d^2\tilde{W}/dh^2=-A_1,\qquad (22)$$

where A_1 is the free parameter required to obtain the limited value of the integral $I(h)=-\frac{h}{n}\int_0^h\frac{\tilde{W}\,dh}{1+n^2h^2}$ for $h\to\infty$. This condition was used only to obtain the logarithmic asymptotic of the mean velocity. The physical sense of the parameter A_1 is a clear, because this parameter is directly proportional to the normal pressure gradient on the wall:

$$\frac{\P\tilde{P}}{\P h}=\frac{2nr}{h}\frac{\P\Phi}{\P h},\ \text{thus}\ \left.\frac{\P\tilde{P}}{\P h}\right|_{h=0}=\frac{2nr}{h}A_1.$$

First and second boundary conditions (22) are following from the definition of $\tilde{W}$.

To minimise the number of the independent random parameters the general solution of the first equation (19) can be written as $\tilde{W}=-(h_t/n)c_1(nh,R_t)$, where

the universal function c_1 depends on the composition of random parameters (the dynamic roughness Reynolds number):

$$R_t = \frac{hh_t}{n(h_x^2 + h_y^2)} \tag{23}$$

and satisfies to the equation

$$(1+x^2)\frac{d^3 c_1}{dx^3} + (R_t c_1 + 2x)\frac{d^2 c_1}{dx^2} = 0 \tag{24}$$

with boundary conditions at

$$x = 0: \quad c_1(0) = 0, \quad dc_1/dx = 1, \quad d^2 c_1/dx^2 = a \tag{25}$$

where $x = nh$, a is also the free parameter required to obtain the limited value of the integral $I(x)$ at $x \to \infty$. Note, that (24) can be derived from the first equation (19). Consequently the integral $I(x)$ depends on the composition of random parameters R_t and can be calculated as

$$I(x, R_t) = \int_0^x \frac{R_t c_1(x, R_t)\, dx}{1+x^2} \tag{26}$$

The integral (26) has been computed in the range $-2.5 \le R_t \le 700$ together with (24-25). Fourth-order scaled Runge-Kutta algorithms and the shooting method have been used to get the numerical solution. Note that for $R_t = 0$ this problem has the analytical solution:

$$c_1(x) = \int_0^x (1 + a\arctan x)dx .$$

In this case $I(x) = 0$, hence one can suggest that function

$$\$(x) = \lim_{R_t \to 0} I(x)/R_t = \int_0^x \frac{c_1(x)\, dx}{1+x^2}$$

has a limited value at $x \to \infty$. It is possible if only $a = -2/p$, thus

$$c_1(x) = \int_0^x (1 - \frac{2}{p}\arctan x)dx$$

This solution has been used as the initial position in the shooting method.

The normalized function $I(x)/R_t$ is shown in Figure 2,a for the various $R_t = -0.83; 0.026; 0.83; 3.32; 26.56$ - the solid lines *1-5* respectively. As it is shown the function $I(x)/R_t$ is simple and smooth function as $\arctan(x)$.

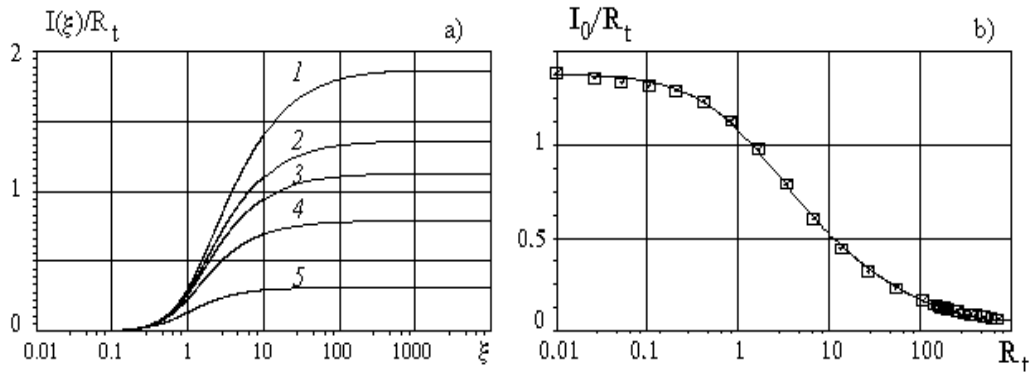

Figure 2: a) The normalised function $I(x)/R_t$ computed on equations (24, 26) for the various $R_t = -0.83; 0.026; 0.83; 3.32; 26.56$ - the solid lines *1-5* respectively; b) The normalised integral $I_0(R_t)/R_t$ depending on the dynamic roughness parameter for $R_t > 0$

The calculated limited value $I_0(R_t) = \lim_{x\to\infty} I(x, R_t)$ is shown in Figure 2,b by the symbols together with the approximated line

$$I_0(R_t)/R_t = 1.38 - 1.13\arctan[0.4\ln(1+R_t{}^q)], \qquad (27)$$

$$q = \begin{cases} 1, & 0 \le R_t \le 100 \\ 1-(1.5R_t - 150)10^{-4}, & 100 < R_t \le 700 \end{cases}$$

To simplifier the numerical modelling of the mean velocity profile over a rough surface the function $I(x, R_t)$ has been approximated as

$$I(x, R_t) \cong \frac{2}{p} I_0(R_t)\arctan[(0.4 + 0.02R_t{}^{3/4})x] \qquad (28)$$

where $I_0(R_t)$ is given by (27).

Finally note that for the negative value of the parameter R_t in the range $R_t < -2.5$ the numerical procedure becomes unstable one. In this case the value $I_0(R_t) = \lim_{x\to\infty} I(x, R_t)$ increases considerably with the small decreasing of the dynamic roughness parameter R_t. Since this branch of the integral $I_0(R_t)$ will not be used in our analysis, therefore data for the negative value $R_t < 0$ is not presented in Figure 2, b and has been neglected in approximation formula (27).

2.7. Mean velocity logarithmic profile in turbulent flow over smooth surface

The turbulent boundary layer over a smooth surface is the best example for the

theoretical consideration and modelling according to the model (21). In this case the streamwise velocity gradient can be written in the standard form using the inner layer variables $z^+ = zu_t / n$, $u^+ = \tilde{u} / u_t$, and boundary conditions for the mean velocity gradient:

$$\text{at } z^+ \to 0 \quad du^+ / dz^+ \to 1;$$

$$\text{at } z^+ \to \infty \quad du^+ / dz^+ \to 1 / k\, z^+,$$

where k is the Karman constant. As it was suggested in subsection 2.1 we have used parameters with stars instead of random parameters. Finally we have got for the streamwise velocity gradient

$$\frac{du^+}{dz^+} = \frac{Ae^{-I}}{1+(z^+ / l^+)^2} + \frac{e^{I_0 - I}}{k l^+ \sqrt{1+(z^+ / l^+)^2}} \tag{29}$$

where $A = 1 - e^{I_0} / k l^+$, $l^+ = hu_t / nn$.

The first term in the right part (29) has the essential value mainly close to the wall (if $A \neq 0$) and the second one gives the main contribution in the logarithmic layer. To derive the mean velocity profile we should firstly defined the parameter $A = 1 - e^{I_0} / k l^+$. Note, from first equation (21) and (29) it follows that

$$A = \cos^2 a \, \frac{du^+(0)}{dz^+} + \cos a \sin a \, \frac{d\,\mathrm{v}^+(0)}{dz^+}$$

where $a = \arctan(h_y / h_x)$, $\mathrm{v}^+ = \tilde{\mathrm{v}} / u_t$. Our suggestion about the dynamical roughness structure is that the parameter a fluctuates around the mean value $a = p/2$. This structure looks like furrows elongated along of the mean flow stream lines in the viscous sublayer (see, for instance, Cantwell, Coles & Dimotakis (1978) where a visualization of the coherent structure in the turbulent boundary layer is presented).

Thus for the mean flow $A = 1 - e^{I_0} / k l^+ = 0$, then the length scale $l^+ = hu_t / nn$ can be found as the solution of the equation

$$kR_t = w_0^+ \exp[I_0(R_t)] \tag{30}$$

where $R_t = l^+ w_0^+$, $w_0 = h_t / nu_t$ is the second scale of the turbulent velocity. For an arbitrary value w_0 the equation (30) has two roots or hasn't any roots and only if $dk / dR_t = 0$ this equation has one root. Hence for the uniqueness of the mean velocity profile should be done

$$\frac{1}{w_0^+} \frac{dk}{dR_t} = \frac{e^{I_0}}{R_t} \frac{dI_0}{dR_t} - \frac{e^{I_0}}{R_t^{\,2}} = 0 \tag{31}$$

The numerical solution of the equation (31) with $I_0(R_t)$ determined from (27) gives $R_t = R_t^* \approx 1.22$ and therefore the predicted values of the turbulent theory

constants are given by $w_*^+ = kR_t^* \exp(-I_0) = 0.14$, $l_0^+ = R_t^* / w_*^+ = 8.71$ for $k = 0.41$. The fundamental parameter of length for the turbulent boundary layer is defined from here: $l_0 = l_0^+ n / u_* \approx 8.71 n / u_*$, that almost coincides with the peak of turbulence production $= \frac{n}{u_t^4}\left(-\langle u'v'\rangle \frac{d\bar{u}}{dz}\right)$, obtained by Klebanoff (1954) and Laufer (1954) - see for instance Rotta (1972) (this book has been kindly indicated by referee).

If $A = 0$ then $l^+ = l_0^+$ in (29) and this equation can be presented in the form:

$$\frac{du^+}{dz^+} = \frac{e^{I_0 - I}}{k\, l_0^+ \sqrt{1 + (z^+ / l_0^+)^2}} \quad , \quad I(z^+ / l_0^+, R_t^*) = \int_0^x \frac{R_t^*\, c_1(x, R_t^*)\, dx}{1 + x^2} \tag{32}$$

Integrated the first equation (32) we have:

$$u^+ = \int_0^{z^+} \frac{e^{I_0 - I} dz^+}{k\, l_0^+ \sqrt{1 + (z^+ / l_0^+)^2}} = \frac{1}{k}\int_0^x \frac{(e^{I_0 - I} - 1)dx}{\sqrt{1 + x^2}} + \frac{1}{k}\int_0^x \frac{dx}{\sqrt{1 + x^2}} =$$

$$\frac{1}{k}\int_0^x \frac{(e^{I_0 - I} - 1)dx}{\sqrt{1 + x^2}} + \frac{1}{k}\ln\left(\frac{z^+}{l_0^+} + \sqrt{1 + \left(\frac{z^+}{l_0^+}\right)^2}\right)$$

The standard logarithmic profile can be derived from here at $z^+ >> l_0^+$:

$$u^+ = \frac{1}{k}\ln z^+ + c_0, \quad c_0 = \frac{1}{k}\int_0^\infty \frac{e^{I_0 - I} - 1}{\sqrt{1 + x^2}} dx \; - \frac{1}{k}\ln\frac{l_0^+}{2}. \tag{33}$$

Therefore, with the given constant k another constant of the mean velocity logarithmic profile can be calculated from (33). It gives $c_0 = 5.015$ for $k = 0.41$.

The velocity profile calculated with (32) for $k = 0.41$; $l_0^+ = 8.71$ is shown in Figure 3, a by the solid line (*1*). The predicted profile (*1*) has been compared with the mean velocity profile computed on the model of the transitional layer proposed by Van Driest (1956), which is shown by the solid line (*2*). As explained by Cebeci & Bradshaw (1984) the Van Driest's model can be written in the form

$$\frac{du}{dz} = \frac{(-\langle u'w'\rangle)^{1/2}}{k\, z[1 - \exp(-z / l_d)]}, \qquad -\langle u'w'\rangle + n\frac{du}{dz} = u_t^2 \tag{34}$$

where l_d is the damping length, $l_d = 26n / u_t$.

The profile computed on (34) coincides with the predicted profile *1* in the viscous sublayer and in the logarithmic layer but differs a bit in the transitional layer (see Figure 3, a). This difference can be explained by the pressure gradient effect. Figure 3,b demonstrates the comparison of both profiles (*1,2*) with several data bases: *3* - the direct numerical simulation of the turbulent flow in the two-dimensional channel ($\mathrm{Re} = 2980$) by Kuroda et al (1989); *4* - the turbulent

boundary layer in zero pressure gradient ($d_0^+ = 406.43$) by Nagano *et al* (1992) and *5* - the turbulent boundary layer mean velocity profile ($\mathrm{Re} = 13052$) presented by Smith (1994). Note that both profiles well correlated with computed and experimental data.

In the upper layer for $z^+ \geq d_0^+$ the mean velocity profile should be constant in contrast to the logarithmic profile which diverges at $z^+ \to \infty$. As it is well known in the outer region of the turbulent boundary layer the mean velocity profile can be described by the defect low $U_0^+ - u^+ = w(z/d_0)$, where the universal function $w = w(z/d_0)$ weakly depends on the Reynolds number and roughness parameters in the case of a zero pressure gradient.

One can suggest that the mixed layer turbulence is generated in the same way as the wall turbulence. Then the new dynamic roughness surface can be introduced and the equation system which is similar to (21) can be derived. In the case of the mixing layer we can put $I = I_0$. With two characteristic scales d_0 and l_0 the general solution for the boundary layer mean velocity profile can be written as (see Trunev (1999))

$$u^+ = e_0 u_{in}^+(z^+) - \frac{e_0}{k}\left(\mathrm{Arsh}(\bar{z}) + \mathrm{Arsh}(\bar{z}_0)\right) + \frac{e\sqrt{1+\bar{z}_0^2}}{k}\left(\arctan\bar{z} + \arctan\bar{z}_0\right) \qquad (35)$$

where $e_0 = 1 + (1-e)/kV_* \,\mathrm{Re}_* \sqrt{1+\bar{z}_0^2} \approx 1 + 0.9/\mathrm{Re}_*$, $\bar{z} = (z - z_0)/V_* d_0$, $z_0 = d_0/2$ is the middle position of the mixing layer, $\bar{z}_0 = z_0/V_* d_0$, $\mathrm{Re}_* = u_t d_0/n$, $u_{in}^+(z^+)$ is the mean velocity profile in the inner layer given by eq. (32), $\mathrm{Arsh}(\bar{z}) = \ln(\bar{z} + \sqrt{1+\bar{z}^2})$.

Profile (35) depends on two dimensionless values which have been defined from experimental data as $V_* = 0.27;\ e = 0.79$. The mean velocity profile and defect low calculated on (35) are shown in Figure 3, c-d, together with experimental data by Nagano et all (1992). Note, that the agreement between theoretical and experimental results in general is good.

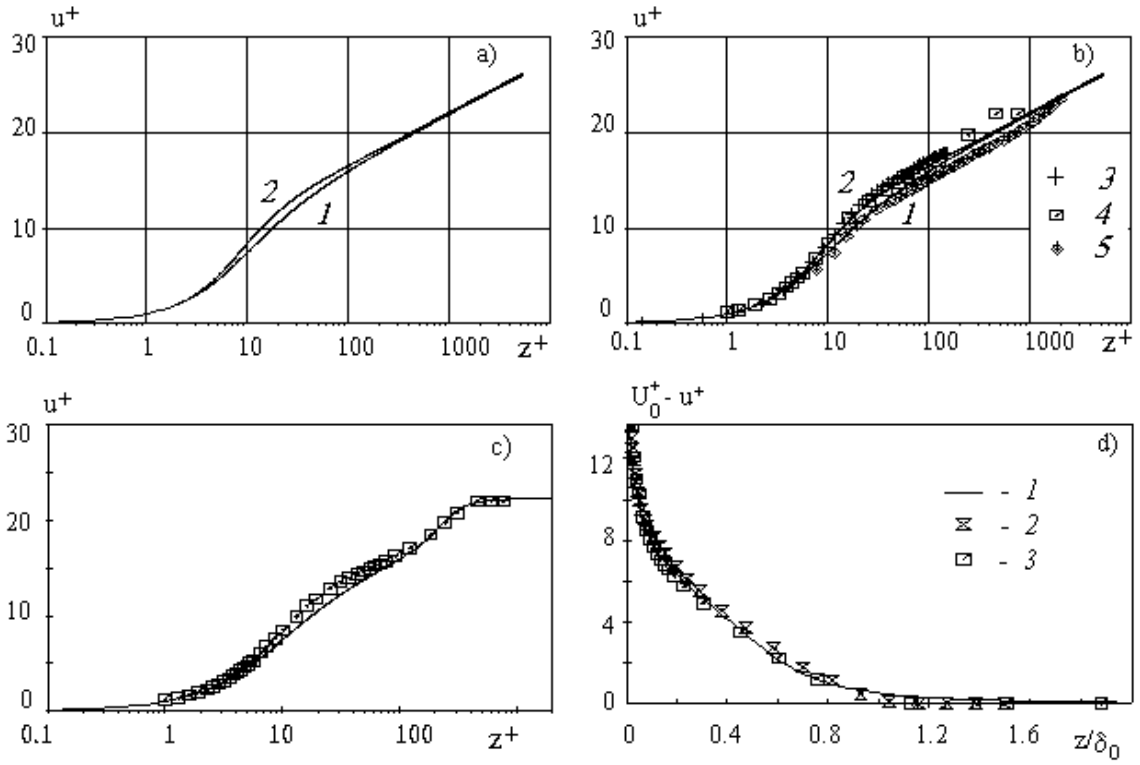

Figure 3. Mean velocity profile in the turbulent boundary layer: a) profiles computed on the present model (*1*) and van Driest model (*2*); b) comparison of computed profiles (*1-2*) with DNS data (*3*) and experimental data (*4-5*); c) the solid line is computed on eq.(35), experimental data Nagano et all (1992) presented by symbols d) defect low: the solid line *1* is computed on eq. (35), *2,3* - experimental data by Nagano et all (1992)

3. Rough surface effect modelling

3.1. Rough surface model

The additive dynamic roughness surface model considered above is given by

$$h(x,y,t) = r(x,y) + h_r(x,y,t)$$

where $h_r(x,y,t)$ is the height of the viscous sublayer over the rough surface. Averaged this equation over a large area $\Delta x \Delta y = L_x L_y$ we have: $\bar{h} = r_a + \bar{h}_r, \bar{h}_t = \bar{h}_{rt}$, where r_a is the mean roughness height,

$$r_a = \frac{1}{L_x L_y} \iint_{\Delta x \Delta y} r(x,y)dxdy$$

After replacing of the origin of the coordinate system in the new position $z \to z - r_a$ the dynamic roughness equation can be written as:

$$h_1(x,y,t) = r(x,y) - r_a + h_r(x,y,t) \tag{36}$$

where $\bar{h}_1 = \bar{h}_r, \bar{h}_{1t} = \bar{h}_{rt}$. Thus, we can imagine the smooth wall located at $z = r_a$ as was defined by Schlichting (1936) and the dynamic roughness surface with dynamic roughness parameters given by (36). For this problem we should suggest that $h_1 > 0$.

Note that the fluid flow near the plane surface $z = r_a$ is a typical heterogeneous flow included two parts: the roughness rigid elements part $S_a = S_a(r_a)$ and the fluid flow part equals to $\Delta S - S_a$, where $\Delta S = L_x L_y$. Put $\Lambda_a = \Delta S / S_a(r_a)$ is the ratio of the whole area $\Delta S = L_x L_y$ to the roughness area $S_a = S_a(r_a)$ at $z = r_a$. The roughness density parameter proposed by Dvorak (1969) is given by $\Lambda_s = \Delta S / S$, where S is the total roughness area. Since $r_a = ak_r / \Lambda_s$, so $\Lambda_a = \Lambda_a(r_a)$ can be considered as a function of the Dvorak's roughness parameter: $\Lambda_a = \Lambda_a(\Lambda_s)$. For the roughness elements considered by Bettermann (1966), Schlichting (1936) and Coleman *et. al.* (1984) this function can be calculated in the closure form.

For the roughness compounds by the spherical uniform elements $r_a = 2k_r / 3\Lambda_s$, $S_a(r_a) = S[1-(1-2r_a / k_r)^2]$, hence

$$\frac{1}{\Lambda_a} = \frac{8}{3\Lambda_s^{\,2}}\left(1 - \frac{2}{3\Lambda_s}\right) \tag{37,a}$$

In the case of the surface roughened by spherical segments (see Figure 1) we have: $r_a = k_r(3 + k_r^{\,2} / r^2) / 6\Lambda_s$, $S_a(r_a) = S(1 + r_a k_r / r^2)(1 - r_a / k_r)$, therefore

$$\frac{1}{\Lambda_a} = \frac{S_a(r_a)}{\Delta S} = \frac{1}{\Lambda_s}\left(1 - \frac{3+e}{6\Lambda_s}\right)\left(1 + \frac{e(3+e)}{6\Lambda_s}\right) \tag{37,b}$$

where, $e = k_r^{\,2} / r^2$.

In the case of the surface with conical uniform elements $S_a(r_a) = S(1 - r_a / k_r)^2$, $r_a = k_r / 3\Lambda_s$, thus

$$\frac{1}{\Lambda_a} = \frac{1}{\Lambda_s}\left(1 - \frac{1}{3\Lambda_s}\right)^2 \tag{37,c}$$

In the case of two dimensional roughness as it has been considered by Bettermann (1966), Dvorak (1969) and Dalle Donne & Meyer (1976) $\Lambda_a = \Lambda_a(r_a)$ depends only on the roughness elements width and pitch (see Figure 1):

$$\Lambda_a = \Lambda_s = L / d \tag{37,d}$$

The mean liquid surface between the roughness elements at $z = r_a$ equals to $(1 - 1/\Lambda_a)\Delta S$, therefore the mean fluid density $\bar{r} = (1 - 1/\Lambda_a) r$ (note that in the real case additionally some liquid volume can be excluding from the mean flow,

hence it can be $\bar{r} = (1 - f / \Lambda_a) r$ where $f \geq 1$ is the shape parameter counted for instance the liquid involved in the viscous sublayer around the roughness elements). The mean dynamic viscosity is defined as $\bar{m} = \bar{r} n = (1 - 1/\Lambda_a) m$.

Thus $\Lambda_a = \Lambda_a(r_a)$ is the important parameter for the rough surface effects modelling because the boundary condition for the mean velocity gradient should be given at $z = r_a$.

3.2. Mean velocity logarithmic profile in turbulent flow over rough surface

The mean velocity logarithmic profile in the turbulent flow over the rough surface can be derived from (32) written in the new coordinate system:

$$\frac{du^+}{dz_1^+} = \frac{\exp(\hat{I}_0 - \hat{I})}{k\, l^+ \sqrt{1 + (z_1^+ / l^+)^2}} \quad , \; \hat{I} = -\frac{h_1}{n} \int_0^{h_1} \frac{\tilde{W} dh_1}{1 + n_1^2 h_1^2} \tag{38}$$

where $z_1 = z - r_a$, $\hat{I}_0 = \lim_{h_1 \to \infty} \hat{I}(h_1)$, $h_1 = z_1 / h_1$, $n_1 = \sqrt{h_{1x}^2 + h_{1y}^2}$.

The boundary condition for the equation (38) on the effective smooth wall is given by

$$\bar{m}\, du / dz_1 = t_a \qquad \text{at} \qquad z_1^+ = 0 \tag{39, a}$$

where t_a is the effective shear stress applied to the effective smooth wall at $z = r_a$. Thus for the dimensionless mean velocity gradient on the effective wall in common case one can propose the equation

$$\bar{m} du^+ / dz_1^+ = \bar{m} G_a = m t_a / t \qquad \text{at} \qquad z_1^+ = 0 \tag{39, b}$$

As it follows from the mean velocity logarithmic profile in the turbulent flow established by Schlichting (see eq. (4)) the dimensionless turbulent length in the first equation (38) depends on the roughness parameters and thus can't be defined from an equation similar to eq. (30). To define l^+ note, that for the completely rough regime in the classical sense, when $k_r^+ >> 1$, one can suppose that $\hat{I} \approx \hat{I}_0$. Then the exact solution of the problem (38-39) can be written as

$$u^+ = \frac{1}{k} \ln\left(k G_a z_1^+ + \sqrt{1 + (k G_a z_1^+)^2} \right) \tag{40}$$

But this equation also follows from (38) if we put $R_t = 0$ in the non-linear model (24), and therefore $\hat{I} = \hat{I}_0 = 0$. Hence, in the case of turbulent flow over a rough surface the main turbulent length scale can be defined as $l^+ = 1/kG_a \neq l_0^+$, and the second scale of the turbulent velocity equals zero.

The mean velocity logarithmic profile follows from (40) at the long distance

from the wall. Put $z_1^+ >> 1/kG_a$ in (40), and then we have

$$u^+ = \frac{1}{k}\ln z_1^+ + c, \text{ where } \quad c = \frac{1}{k}\ln(2kG_a).$$

This equation can be rewritten in the standard form as follows:

$$u^+ = \frac{1}{k}\ln z_1^+ + c_0 - \frac{1}{k}\ln k_r^+ - D(\Lambda_s), \quad D(\Lambda_s) = c_0 + \frac{1}{k}\ln\frac{1}{2kk_r^+G_a} \tag{41}$$

where $c_0 = 5.015$. Note, that the finale result (41) mainly depends on the mean velocity gradient applied to the effective smooth surface at $z_1^+ = 0$.

3.3. Roughness density effect model

There are two available cases which can be realised in the experimental situation: the roughness elements installed on the absolutely smooth surface and the roughness elements installed on the rough surface. In the first case we surmise that the mean velocity gradient applied to the effective smooth wall is proportional to the velocity gradient over a smooth surface given by the first equation (32) for $z = r_a$. Used the boundary condition (39,b) we have:

$$(1 - f/\Lambda_a)G_a = \frac{t_a}{t} = \frac{b\exp[I_0 - I(r_a^+)]}{kr_a^+\sqrt{1+(l_0^+/r_a^+)^2}} \tag{42}$$

where the shape parameter $f \geq 1$ introduced to estimate the frontal and leeward re-circulation zones effect, $r_a^+ = r_a u_t / n$, b is the parameter. Suggested that $b/\sqrt{1+(l_0^+/r_a^+)^2} = b_0$ where b_0 is a function of the roughness parameters, we have (for the smooth background surface):

$$(1 - f/\Lambda_a)G_a = \frac{b_0 g}{kr_a^+}, \qquad g = \exp[I_0 - I(r_a^+)] \tag{43}$$

here g is the transitional layer parameter. Note, that for the high value of the roughness density parameter may be $k_r^+ >> 1$ (completely rough regime in the classical sense), but simultaneously $r_a^+ = ak_r^+/\Lambda_s \leq 1$. Thus $g = 1$ for the completely rough regime (in the non-classical sense) defined only for $r_a^+ >> l_0^+$ as it follows from the second equation (43). The main turbulent length scale can be estimated from (43) as $l^+ = 1/kG_a = r_a^+(1 - f/\Lambda_a)/b_0 g$.

Substituted G_a from (43) into the second equation (41) finally we have:

$$D(\Lambda_s) = c_0 + \frac{1}{k}\ln\frac{a(1 - f/\Lambda_a)}{2b_0\Lambda_s} - \frac{\ln g}{k} \tag{44}$$

The rough surface effect model (44) depends on two parameters b_0, f chosen from the best correlation with the experimental data. We should underlined that b_0 is the friction parameter of the rough surface and f is the parameter of the mean density of fluid involved in the mean turbulent flow at the level $z = r_a$.

In the second case the mean velocity gradient model is the same as (44) but we should put $r_a = ak_r / \Lambda_s + r_g$ where r_g the averaged height of the background roughness is. Both models have been testified and shown the good agreement with the experimental data.

3.4. Modelling of roughness density effect. 3D roughness elements

To test the roughness surface effect model (44) the turbulent flow data for 3D roughness elements obtained by Schlichting (1936) and re-evaluated by Coleman *et. al*. (1984) has been used. The main result reported by Coleman *et. al*. (1984) is that some Schlichting's data was obtained probably in the transitionally rough regime. The experimental techniques in Schlichting's (1936) and Coleman *et. al*. (1984) experiments have been analyzed and it was surmised that Schlichting's data was measured in the fully rough regime but some details of his experimental technique have not been reported.

The computed (*1*) and experimental data by Schlichting (*3*) and Coleman *et. al*. (*5*) are shown in Figure 4 for spheres (Fig. 4,a), spherical segments (Fig. 4,b) and cones (Fig. 4,c). The points (*4*) are computed from the experimental data by Coleman *et. al*. (*5*) which has been corrected with transitional layer parameter g calculated on (27-28) as follows $g = \exp[1.264 - 0.805\arctan(0.048 r_a^+)]$. As it is shown in Figure 4 the transitional layer effect is essential for the plate with roughness in a form of spherical segments (two points with $k_r^+ = 14; 27$ and consequently $\Lambda_s = 31.8; 17.9$) and conical elements (two points with $k_r^+ = 55; 211$ and $\Lambda_s = 31.8; 17.9$ respectively), and relatively small for all data with $r_a^+ = ak_r^+ / \Lambda_s \geq 16$, including data for the plate roughened by spheres. Note, that the experimental data re-evaluated by Coleman *et. al*. (1984) is getting closer to the original Schlichting's data after the correction on the transitional layer effect. Therefore it seems to be clear that the data by Coleman *et. al*. (1984) is rather based on another experimental technique then the original Schlichting's data.

The corrected data has been used to estimate the parameters b_0, f in the equation (44) which can be written for the completely roughness regime ($g = 1$) as follows

$$D(\Lambda_s) = c_0 + \frac{1}{k}\ln\frac{a(1 - f/\Lambda_a)}{2b_0\Lambda_s} \qquad (45)$$

where the roughness parameters $a, \Lambda_a = \Lambda_a(r_a)$ are given by (37, a-c) for the spheres, spherical segments and conical elements respectively.

As it has been established in the case of the plate with spheres $b_0 = 0.65$, $f = 1.11$ for the data obtained by Coleman *et. al.* (1984) (solid line (*1*) in Figure 4,a) and $b_0 = 0.4$, $f = 1.25$ for the corrected points. For the roughness elements in the form of spherical segments $b_0 = 3$, $f = 1$ (solid line (*1*), Figure 4,b) and for the conical elements $b_0 = 0.7$, $f = 1$ - see Figure 4,c. For comparison the Bettermann-Dvorak's correlated line (*2*) also is shown in Figure 4.

The magnitude b_0 can be explained in terms of the rough surface drag which has the same value for the spheres and conical elements and mach less for the surface with spherical segments. The mean fluid density parameter is $f \approx 1$ for considered types of roughness elements. Note that in the case of the surface roughened by spheres the function $D(\Lambda_s)$ has a maximum at $\Lambda_s \approx 2.35$ (as has been established in numerical experiments the maximum location depends on the value f approximately as $\Lambda_s \approx 2.175 f^{2/3}$ for the range $1 \le f \le 2$).

The experimental data for the surfaces with spheres, spherical segments or conical elements can be collected together used an "universal" parameter wich is different from that proposed by Bettermann (Dvorak (1969), Dirling (1973), Simpson (1973), Kind & Lawrysyn (1992) and other. This correlation is available for the high roughness density parameter at $\Lambda_s >> 1$, then

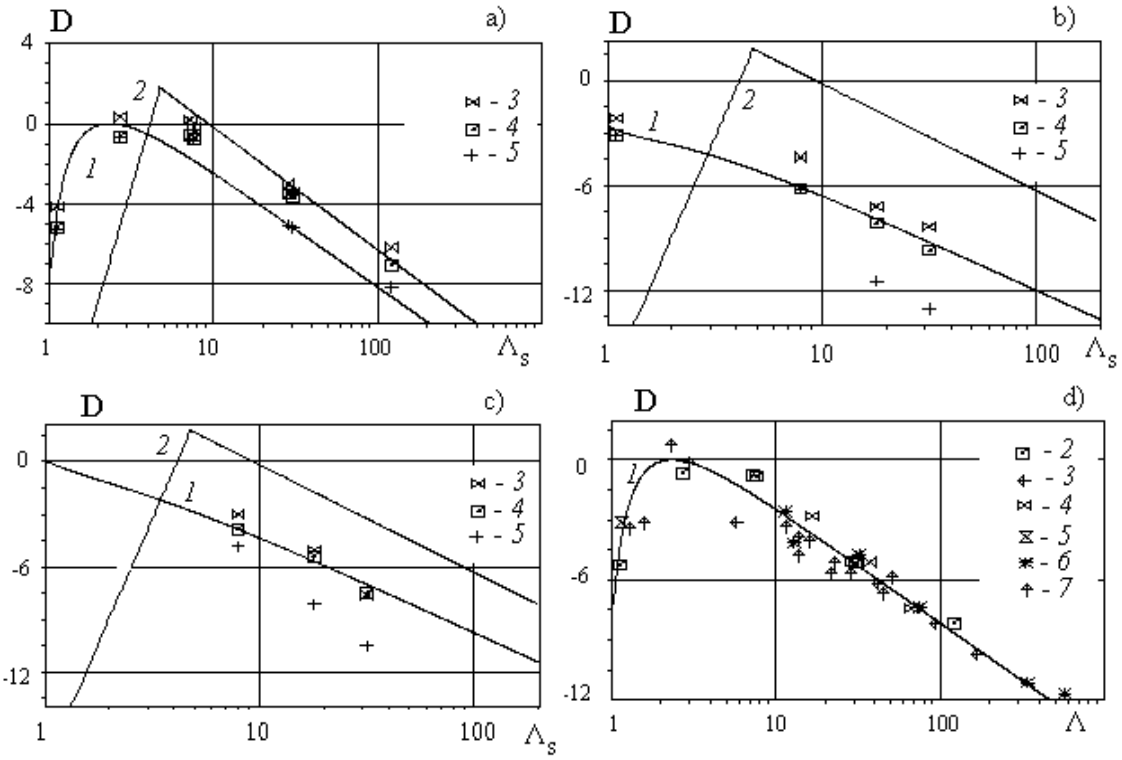

Figure 4. Roughness density effect on the turbulent flow in a case of 3D roughness elements: a) spheres; b) spherical segments; c) cones; d) the generalised correlation

$$D(\Lambda_s) \approx c_0 + \frac{1}{k} \ln \frac{a}{2b_0 \Lambda_s}$$

and therefore the "universal" parameter is given by $\Lambda = b_0 \Lambda_s / a$. The solid line (*1*) computed on the equations (37,a), and (45) for $b_0 / a = 1$, $f = 1.11$ is shown in Figure 4, d with the corrected experimental data for the rough surfaces with spheres (*2*), spherical segments (*3*) and conical elements (*4*) . The classic sand grain-roughened pipe flow experiment of Nikuradse (1933) with $D = -3, \Lambda_s = 4/p$ is presented by point (*5*). The hoar-frost roughness data of Kind & Lawrysyn (1992) is plotted by points (*6*). Note, that data of Kind & Lawrysyn (1992) has been corrected with transitional layer parameter

$$g = \exp[1.264 - 0.805 \arctan(0.048 r_a^+)] / (1 + \Lambda_s r_g / a k_r)$$

where $r_a = a k_r / \Lambda_s + r_g$, $a = 1/3$, $r_g = k_r f_r$ is the averaged height of the background roughness, f_r depends on the frost formation and has been calculated for the plate 1-6 of Kind & Lawrysyn (1992) as follows $f_r = 0.013; 0.04; 0.12; 0.12; 0.04; 0.04$. In this case $b_0 = 0.7$ as for the conical elements. The experimental data for 3D roughness elements of Simpson (1973) is shown by symbols (*7*). For his data $0.45 \le b_0 / a \le 0.55$.

Thus one can suggest that the rough surface with spheres is the basic case for 3D roughness elements, because all data shown in the Figure 4, d is correlated well with the basic line (*1*).

Then one can propose the model for b_0 considered this parameter as a function of the width-to-height ratio $b_0 = b_0(d / k_r)$. For instance, at $b_0 / a = 1$ we have the Dvorak's roughness density parameter $\Lambda = \Lambda_s = \Delta S / S$. For a linear function $b_0 = b_0(d / k_r)$ the "universal" parameter is related to that of Bettermann (1966) since in the case of transverse square bars $S = d, a = 1$ and hence $\Lambda = b_1 L / k_r$, where b_1 is the numerical value.

3.5. Modelling of roughness density effect. 2D roughness elements

The empirical model of Dalle Donne & Meyer (1977) for 2D roughness composed by the transverse rectangular rods is based on the roughness density parameter

$$\Lambda_D^* = (L-d)/k_r = (d/k_r)(\Lambda_s - 1)$$

With this parameter the experimental data of Dalle Donne & Meyer (1977) and other sources summarized in Table I can be described as follows

$$D(\Lambda_D^*) = c_0 + (2+7/\Lambda_D^*)\lg\frac{k_r}{d} - R, \quad R = \begin{cases} 9.3(\Lambda_D^*)^{-0.73}, 1 \le \Lambda_D^* \le 6.3 \\ 1.04(\Lambda_D^*)^{0.46}, 6.3 \le \Lambda_D^* \le 160 \end{cases} \qquad (46)$$

This correlation has been derived by Dalle Donne & Meyer (1977) for the range of the experimental data parameters $0.086 \le k_r/d \le 5.0$ and $1.85 \le \Lambda_s \le 980$.

As it is shown (see (46)) the rough surface effect depends on two roughness parameters k_r/d and Λ_D^*. Thus, there is no any "universal" parameter for 2D roughness elements in the common case. But the experimental data with various k_r/d can be plotted together as the graph of the function $D_1(\Lambda_D^*) = D(\Lambda_D^*) - (2+7/\Lambda_D^*)\lg(k_r/d)$. Figure 5 demonstrates $D_1(\Lambda_D^*)$ calculated according to (46) - solid line (*1*) and the experimental data found for 2D roughness elements by various authors listed in Table 1 (the corrected and reduced data or $R(\infty)_{01}$ from Table 2 of Dalle Donne & Meyer (1977) has been used as long as correlation (46) was proposed for this values).The symbols description is given in the right part of Figure 5 and Table 1. As it is shown the correlation is good for the middle and high value of the roughness density parameter, but for $\Lambda_D^* \approx 1$ the scatter of the points is rather large and can't be explained by the experimental technique differences only.

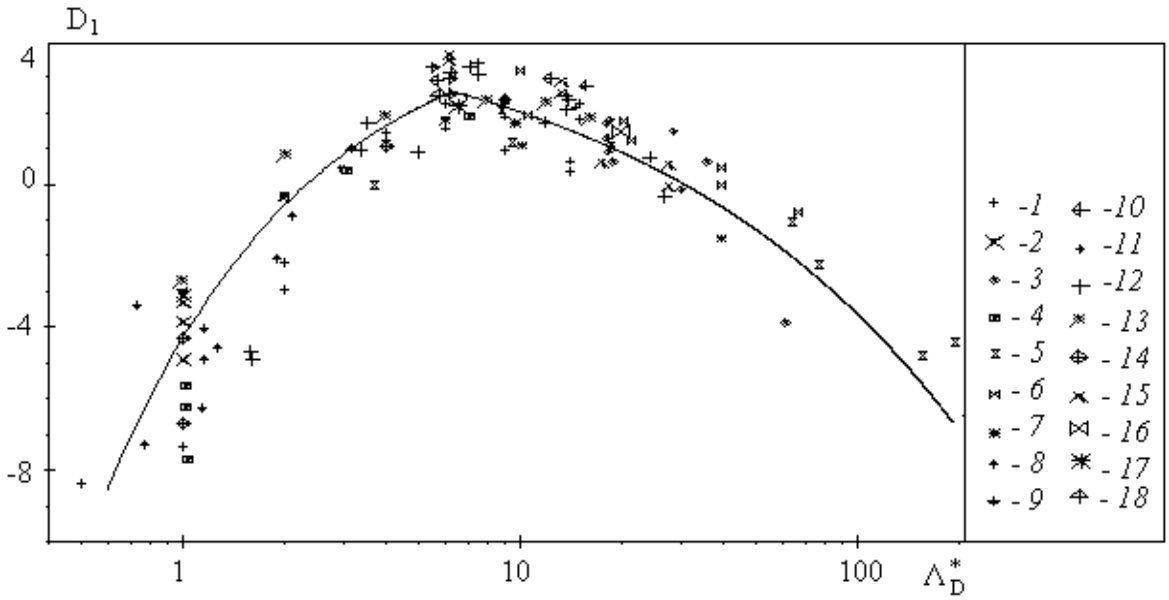

Figure 5: D_1 vs Λ_D^* - the solid line. 2D roughness elements data *1-18* has been obtained by authors listed in Table 1

Table 1.

Authors	Year	Geometry	L/d	k_r/d	Symbol
Möbius	1940	Tube	10.0-29.22	0.3-2.20	3
Chu & Streeter	1949	Tube	1.95-7.57	0.93	4
Sams	1952	Tube	2.0-2.3	0.88-1.37	9
Nunner	1956	Tube	16.36	0.8	16
Koch	1958	Tube	9.8-980	1.0-5.0	5
Fedynskii	1959	Annulus	6.67-16.7	1.0	10
Draycott & Lawther	1961	Annulus	2.0	1.0	2
Skupinski	1961	Annulus Tube	2.0-41.0 22.2-133.4	1.0 2.0	6
Savage & Myers	1963	Tube	3.66-43.72	1.33-2.67	13
Perry & Joubert	1963	Wind tunnel	4.0	1.0	19
Sheriff, Gumley & France	1963	Annulus	2.0-10.0	1.0	14
Gargaud & Paumard	1964	Tube Annulus	1.8-16.0 10.0-16.0	1.0-1.67 1.0	1
Bettermann	1966	Wind tunnel	2.65-4.18	1.0	20
Massey	1966	Annulus	7.53-30.15	1.06	15
Kjellström & Larson	1967	Annulus	2.02-38.52	0.086-4.08	12
Fuerstein & Rampf	1969	Annulus	2.91-25.04	0.42-2.50	8
Lawn & Hamlin	1969	Annulus	7.61	1.0	17
Watson	1970	Annulus	6.49-7.22	1.0	11
Stephens	1970	Annulus	7.20	1.0	18
Webb, Eckert & Goldstein	1971	Tube	9.70-77.63	0.97-3.88	7
Antonia & Luxton	1971	Wind tunnel	4.0	1.0	21
Antonia & Wood	1975	Wind tunnel	2.0	1.0	22
Dalle Donne & Meyer	1977	Annulus	4.08-61.5	0.25-2.0	24
Pineau, Nguyen, Dickinson & Belanger	1987	Wind tunnel	4.0	1.0	23

Using the roughness density parameter model in the form (37, d) and suggesting that $g = 1$ (completely rough regime) one can write (44) for this case as follows

$$D(\Lambda_s) = c_0 + \frac{1}{k}\ln\frac{(1-f/\Lambda_s)}{2b_0\,\Lambda_s} \qquad (47)$$

For the constant value of the parameters b_0, f the function $D(\Lambda_s)$ has a maximum at $\Lambda_s = 2f$. This maximum can be defined from (46) as $\Lambda_s = 6.3k_r/d + 1$, and therefore $f = (6.3k_r/d + 1)/2$. Thus as it follows from the experimental data the shape parameter varies with k_r/d. To compare the experimental data with the arbitrary value of the shape parameter let us introduce the roughness density parameter in the form $\Lambda_f = \Lambda_s / f$, then the roughness density effect model (47) can be rewritten as

$$D(\Lambda_f) = c_0 + \frac{1}{k}\ln\frac{(1-1/\Lambda_f)}{2b_1\,\Lambda_f} - \frac{1}{k}\ln(df/k_r) \qquad (48)$$

where $b_1 = b_0 k_r / d$.

In this model the experimental data for various k_r/d can be plotted together as the graph of the function $D_f(\Lambda_f) = D(\Lambda_f) + 1/k\,\ln(df/k_r)$ as well as in the Dalle Donne & Meyer's model (46). But as it has been established the shape parameter derived from the model (46) isn't a good approximation.

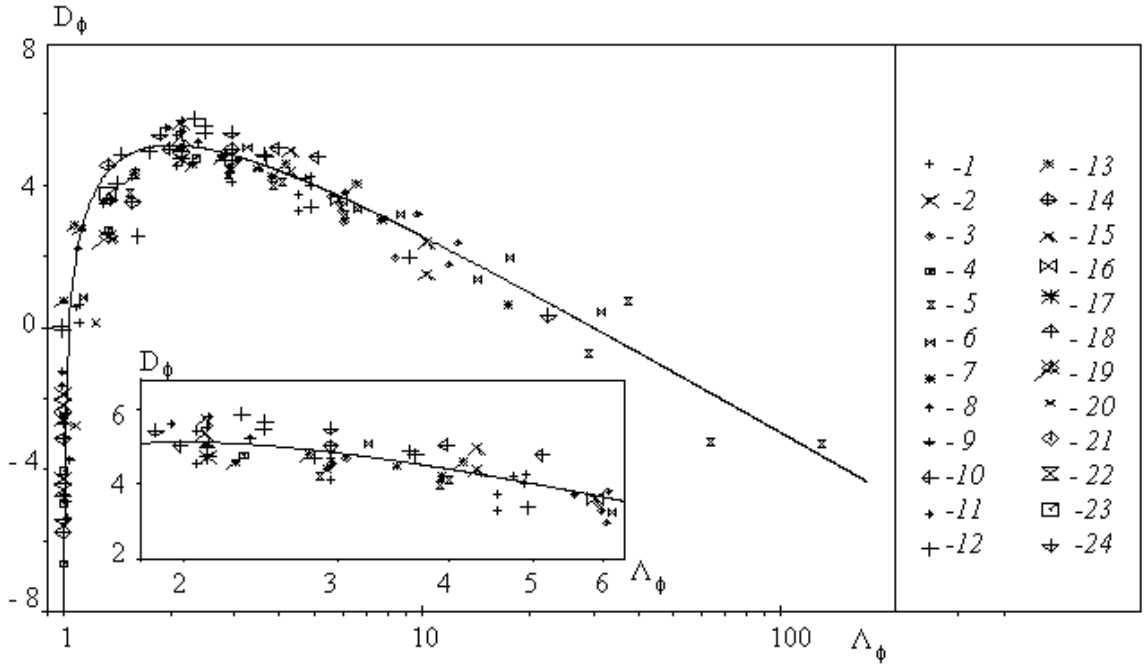

Figure 6: D_f vs Λ_f - the solid line. 2D roughness elements data *1-24* has been obtained by authors listed in Table 1

Note that in the common case one can suggest that $f = 1 + f_1 k_r / d$, where $f_1 k_r$ is the total length of the frontal and leeward re-circulation zones. The model (46) gives for this parameter the unphysical result $f_1 = 3.15 - d/2k_r$. Thus the experi-

mental data of various authors listed in Table 1 has been used to find the right form of f and b_0. The best correlation for about 130 points is given by

$$f = 1 + f_1 \frac{k_r}{d}, \quad f_1 = \exp(-B^{q_1} \ln B^{1/q_1}), \quad b_0 = b_1 \frac{d}{k_r} \tag{49}$$

where $B = (1 + k_r / d) / \Lambda_s$, $q_1 = 0.625$, $b_1 = 0.12$.

Figure 6 shows $D_f(\Lambda_f)$ calculated on (48-49) - the solid line (*1*), and the experimental data *1-24* of various authors listed in Table 1 (note, we have used values $R(\infty)$ from Table 2 of Dalle Donne & Meyer (1977) instead of the original data *1-18*). The symbols description is given in the right part of Figure 6 and in Table 1. A fragment of the correlated line is shown in the lower part of Figure 6. One can see that the predicted roughness density effect (the solid line) is in a good agreement with the available experimental data.

Finally note that formulas (49) are derived for the rough surface composed by the transverse rectangular rods and can't be applied to 2D roughness elements of another form without additionally verification.

3.6. Model of the total length of the frontal and leeward re-circulation zones

Analyzing expression (48) one can find two singular points: $\Lambda_f \to 1$, and $\Lambda_f \to \infty$, which correspond to two branches of function $D_f(\Lambda_f)$. Dalle Donne & Meyer (1977) model (46) also has two singular points $\Lambda_D^* \to 0$ and $\Lambda_D^* \to \infty$. Taken into account that $\Lambda_D^* = (d / k_r)(\Lambda_s - 1)$ one can conclude that these two singular points are located at $\Lambda_s \to 1$ and $\Lambda_s \to \infty$ accordingly. As we can see from the data shown in Figures 5 there is probably another singular point at $\Lambda_D^* \approx 1$. The data collected around the point at $\Lambda_D^* \approx 1$ has been obtained mainly for $k_r / d = 1$. Thus this point can be at $\Lambda_s \approx 2$. But generally speaking what is the physical reason for this point? In Figure 7a the normalised total length of the frontal and leeward re-circulation zones (solid lines) which depends on the Dvorak's roughness density parameter $f_1 = f_1(\Lambda_s)$ and the mean fluid density (broken line) calculated for $k_r / d = 0.5; 2; 5$ are shown.

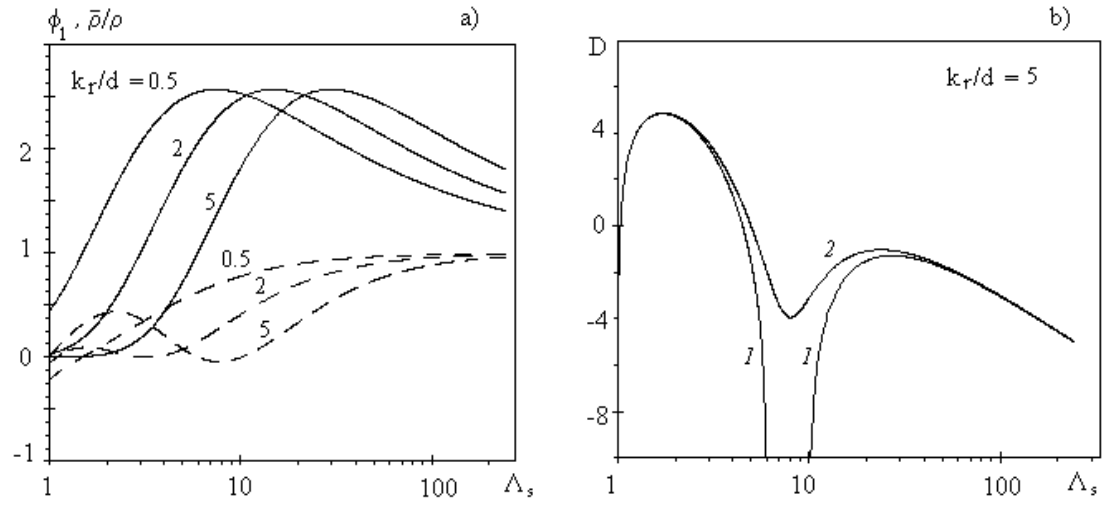

Figure 7. a) The normalised total length of the frontal and leeward re-circulation zones, $f_1 = f_1(\Lambda_s)$ (solid lines), and the normalised mean fluid density as a function of the Dvorak's roughness density parameter (broken lines), calculated for $k_r / d = 0.5;\ 2;\ 5$.

b) The roughness density effect on the shift of the mean velocity logarithmic profile, $D = D(\Lambda_s)$, at fixed $k_r / d = 5$: the solid line *1* is calculated according to model (45)-(49), The solid line *2* is calculated on (47), (49) where f_1 was decreased on 10%

As we can see from Figure 7a the total length has a maximum located in a point $\Lambda_s^* = \Lambda_s^*(k_r / d)$. According to this the effective mean fluid density has a minimum which may be less then zero. As it follows from (39, b), if t_a is limited value and $\overline{m} \to 0$ then $G_a \to \pm\infty$ thus it is a singular point for the function $D = D(\Lambda_s)$. Physically it means that the frontal and leeward re-circulation zones have intersection. As it is well known in this case the skimming flow is realised. In the model (49) this regime is counted statistically and probably with some error. In any case the data over the point $\Lambda_D^* \approx 1$ in Figure 5 is replaced to the point $\Lambda_f = 1$ in Figure 6. Note that correlated line goes throughout this data better in Figure 6 than in Figure 5.

An unexpected result has been found out in numerical experiment that function $D = D(\Lambda_s)$ has one maximum for $k_r / d < 1.436$ and two maximum for $k_r / d \geq 1.436$ as shown by the solid lines *1* in Figure 7b calculated for $k_r / d = 5$. This result is very sensitive to the variations of the value f_1. If f_1 is multiplied by 0.9 then the function $D = D(\Lambda_s)$ louses the singular point and looks like solid line *2* in Figure 7. Now we have only experimental data shown in Figure 7 which is not sufficient to confirm this result.

A restriction for this model can be established if the length scale $l^+ = r_a^+(1-f/\Lambda_a)/b_0 g$ found out for the rough surface is compared with the main turbulent length scale l_0^+ computed for the boundary layer over a smooth surface as $l^+ \geq l_0^+$. It puts the limitation for the normalised mean fluid density as $(1-f/\Lambda_a) \geq l_0^+ b_0 / r_a^+ \approx 1/r_a^+$ for 2D roughness considered above. If this restriction is broken then it means that the model (48)-(49) also can't be used properly. Supposed that in this case $l^+ = l_0^+$ one can regularise the function $D = D(\Lambda_s)$ in the singular point shown in Figure 7,b.

4 Conclusion

The turbulent boundary layer model has been derived directly from the Navier-Stokes equation. The model is based on the special type of the Navier-Stokes equation transformation and thus this model doesn't need in any closures for the Reynolds stresses. The model has been testified in the case of the turbulent flow over smooth surface. The roughness density effect model with the transitional regime parameter has been proposed. With this parameter the equivalent sand roughness data obtained by Coleman *et. al*. (1984) has been corrected in the case of turbulent flow over the surfaces with spherical segments and cones. After correction this data became very close to the original Schlichting's results.

In the case of 2D roughness elements the experimental data bases published by many authors have been analysed and the re-circulation zones total length parameter has been proposed. The rough surface effect on the turbulent flow is calculated. The agreement between computed outcomes and experimental data in general is good.

Acknowledgements

Thanks are due to Prof. F. H. Busse of University of Bayreuth and several anonymous referees of the *Journal of Fluid Mechanics*, for helpful discussion on various aspects of this work.

References

1. Antonia, R.A. & Luxton, R.E. 1971 The Response of a Turbulent Boundary Layer to a Step Change in Surface Roughness, Pt. 1. Smooth to Rough. *J. Fluid Mech.*, **48**, 721-762.
2. Antonia, R.A. & Wood, D.H. 1975 Calculation of a Turbulent Boundary layer Downstream of a Step Change in Surface Roughness. *Aeronautical Quarterly*, **26**, 3, 202-210.
3. Bettermann, D. 1966 Contribution a l'Etude de la Convection Force Turbulente le Long de Plaques Regueuses. *Int. J. Heat and Mass Transfer*, **9**, 153.
4. Cantwell, B. J., Coles D. & Dimotakis, P. 1978 Structure and entrainment in the plane of symmetry of a turbulent spot, *J. Fluid Mech.*, **87**, 641-672.

5. Cebeci, T. & Bradshaw, P. 1984 Physical and Computational Aspects of Convective Heat Transfer, Springer-Verlag, NY.
6. Chu, H. & Streeter, V.L. 1949 Fluid flow and heat transfer in artificially roughened pipes. *Illinois Inst. of Tech. Proc.* No. 4918.
7. Clauser, F. 1956 The Turbulent Boundary Layer. *Advances in Applied Mechanics*, vol**. 4,** pp.1-51.
8. Coleman, H. W., Hodge, B. K. & Taylor, R. P. 1984 A Revaluation of Schlichting's Surface Roughness Experiment. *J. Fluid Eng.* **106**, 3.
9. Data-Base on Turbulent Heat Transfer/ Nagano Y., Kasagi N., Ota T., Fujita H., Yoshida H., Kumada M. Department of Mechanical Engineering, Nagoya Institute of Technology, Nagoya. DATA No. FW BL004.
10. Dirling, R.B., Jr. 1973 A Method for Computing Roughwall Heat-Transfer Rate on Re-Entry Nose Tips. *AIAA Paper*, 73-763.
11. Draycott, A. & Lawther, K.R. 1961 Improvement of fuel element heat transfer by use of roughened surface and the application to a 7-rod cluster. In *Int. Dev. Heat Transfer*, Part III, pp. 543-52, ASME, NY.
12. Donne, M. & Meyer, L. 1977 Turbulent Convective Heat Transfer from Rough Surfaces with Two-Dimensional Rectangular Ribs. *Int. J. Heat Mass Transfer*, Vol. **20**, pp. 583-620.
13. Driest, E.R. Van . 1956 On turbulent flow near a wall. *J. Aero. Sci.* **23**, 1007.
14. Dvorak , F. A. 1969 Calculation of Turbulent Boundary Layer on Rough Surface in Pressure Gradient. *AIAA Journal* **7**, 9.
15. Fedynskii, O. S. 1959 Intensification of heat transfer to water in annular channel. In *Problemi Energetiki*, Energ. Inst. Akad. Nauk USSR (in Russian).
16. Fuerstein, G. & Rampf, G. 1969 Der Einfluß rechteckiger Rauhigkeiten auf den Wärmeübergang und den Druckabfall in turbulenter Ringspaltströmung. *Wärme- und Stoffübertragung*, 2 (1), 19-30.
17. Gargaud, I. & Paumard, G. 1964 Amelioration du transfer de chaleur par l'emploi de surfaces corruguees. CEA-R-2464.
18. Grabov, R.M. & White, C.O. 1975 Surface Roughness Effects on Nose Tip Ablation Characteristics, *AIAA Journal*, **13**, pp. 605-609.
19. Jackson, P.S. 1981 On the displacement height in the logarithmic wind profile. *J. Fluid Mech.*, **111**, 15-25.
20. Kind, R. J. & Lawrysyn, M. A. 1992 Aerodynamic Characteristics of Hoar Frost Roughness. *AIAA Journal* **30**, 7, 1703-7.
21. Kjellström, B. & Larsson, A. E. 1967 Improvement of reactor fuel element heat transfer by surface roughness. AE-271. Data repoted by Dalle Donne & Meyer (1977).
22. Klebanoff, P. S. 1954 Characteristics of turbulence in a boundary layer with zero pressure gradient. *NACA Tech. Note*, **3178**.
23. Koch, R. 1958 Druckverlust und Wärmeübergang bei verwirbelter Strömung. *ForschHft. Ver. Dt. Ing.* 469, Series B, **24**, 1-44.
24. Kuroda, A., Kasagi, N. & Hirata, M. 1989 A direct Numerical Simulation of the Fully Developed Turbulent Channel Flow. In *International Symposium on Computational Fluid Dynamics*, Nagoya, pp. 1174-1179.
25. Laufer, J. 1954 The structure of turbulence in fully developed pipe flow. *NACA Tech. Note* **2954**.
26. Lawn, C. J. & Hamlin, M. J. 1969 Velocity measurements in roughened annuli. CEGB RD/B/N 2404, Berkley Nuclear Laboratories.
27. Massey, F.A. 1966 Heat transfer and flow in annuli having artificially roughened inner surfaces. Ph. D. Thesis, University of Wisconsin.

28. Monin, A.S. & Yaglom, A.M. 1965 *Statistical Fluid Mechanics: Mechanics of Turbulence*. The MIT Press.
29. Möbius, H. 1940 Experimentelle Untersuchung des Widerstandes und der Gschwindig-keitsverteilung in Rohren mit regelmäßig angeordneten Rauhigkeiten bei turbulenter Strömung. *Phys. Z.* **41**, 202-225.
30. Nagano, Y.& Tagawa, M. 1991 Turbulence model for triple velocity and scalar correlation. In Turbulent Shear Flows 7 (F. Durst, B. E. Launder, W. C. Reynolds, F. W., Schmidt, J. H. Whitelaw, eds), Springer, Berlin, Heidelberg, New York , pp. 47-62.
31. Nagano, Y., Tagawa M. & Tsuji. T. 1992 Effects of Adverse Pressure Gradients on Mean Flows and Turbulence Statistics in a Boundary Layer. *8th Symposium on Turbulent Shear Flows proceedings.*
32. Nikuradse, J. 1933 Strömungsgesetze in Rauhen Rohren. *ForschHft. Ver. Dt. Ing.* 361.
33. Nunner, W. 1956 Wärmeübergang und Druckabfall in rauhen Rohren. *ForschHft. Ver. Dt. Ing.* 455.
34. Osaka, H. & Mochizuki, S. 1989 Mean Flow Properties of a d-type Rough Wall Boundary Layer in a Transitionally Rough and a Fully Rough Regime. *Trans. JSME* ser. B, Vol.**55**, No.511, 640-647.
35. Perry, A.E. & Joubert, P.N. 1963 Rough-Wall Boundary Layers in Adverse Pressure Gradients. *J. Fluid Mech.*, **17**, 2, 193-211.
36. Pineau, F., Nguyen, V. D., Dickinson, J. & Belanger, J. 1987 Study of a Flow Over a Rough Surface with Passive Boundary-Layer Manipulators an Direct Wall Drag Measurements. *AIAA Paper*, 87-0357.
37. Prandtl, L. 1933 Neuere Ergebnisse der Turbulenzforschung. *VDI -Ztschr*. **77**, 5, 105.
38. Raupach, M.R. 1992 Drag and drag partition on rough surfaces, *Boundary Layer Meteorol.*, **60,** 375-395.
39. Pulliam, T. H. & Steger, J. L. 1980 Implicit Finite-Difference Simulations of three-dimensional Compressible Flow, *AIAA Journal* **18**, 2, 159.
40. Rotta, J.C. 1972 Turbulente Stromungen. Eine Einfuhrung in die Theorie und ihre Anwendung. B. G. Teubner Stuttgart. P. 156.
41. Sams, E.W. 1952 Experimental investigation of average heat transfer and friction coefficients for air flowing in circular tubes having square-thread-type roughness. NACA RME 52 D 17.
42. Savage, D.W. & Myers, J.E. 1963 The effect of artificial surface roughness on heat and momentum transfer. *A.I.Ch.E.J.*, **9**, 694-702.
43. Schlichting, H. 1936 Experimentelle Untersuchungen zum Rauhigkeits-problem. *Ing.-Arch* **7**(1), 1-34.
44. Schlichting, H. 1960 Boundary Layer Theory. McGraw-Hill, NY, p.527.
45. Sheriff, N., Gumley, P. & France, J. 1963 Heat transfer characteristics of roughened surfaces. UKAEA, TRG Report 447 (R).
46. Sigal, A & Danberg, J.E. 1990 New Correlation of Roughness Density Effect on the Turbulent Boundary Layer. *AIAA Journal*, **25**, 3, 554-556.
47. Simpson, R. L. 1973 A Generalized Correlation of Roughness Density Effect on the Turbulent Boundary Layer. *AIAA Journal* **11**, 9, 242-244.
48. Skupinski, E. 1961 Wärmeübergang und Druckverlust bei künstlicher Verwirbelung und künstlicher Wandrauhigkeiten. Diss. Techn. Hochschule Aachen.
49. Smith, R.W. 1994 Effect of Reynolds Number on the Structure of Turbulent Boundary Layers. Ph.D. Thesis, Princeton University, Princeton, NJ.
50. Stephens, M. J. 1970 Investigations of flow in a concentric annulus with smooth outer wall and rough inner wall. CEGB RD/B/N 1535, Berkley Nuclear Laboratories.

51. Trunev, A. P. 1995 Diffuse processed in turbulent boundary layer over rough surface. In *Air Pollution III, Theory and Simulation* (ed. H. Power, N. Moussiopoulos & C.A. Brebbia). Comp. Mech. Pub. Southampton-Boston.
52. Trunev, A. P. 1996 Similarity theory for turbulent flow over natural rough surface in pressure and temperature gradients. In *Air Pollution IV, Monitoring, Simulation and Control*, (ed. B. Caussade, H. Power & C.A. Brebbia). Comp. Mech. Pub. Southampton-Boston.
53. Trunev, A. P. 1997 Similarity theory and model of diffusion in turbulent atmosphere at large scales. In *Air Pollution V, Modelling, Monitoring and Management.* (ed. H. Power, T. Tirabassi & C .A. Brebbia) Comp. Mech. Pub. Southampton-Boston.
54. Trunev, A. P. & Fomin, V.M. 1985 Continual model of impingement erosion. *J. Appl. Mech. and Tech. Phys.*, **6**, pp. 113-120.
55. Trunev, A. P. 1999 Theory of Turbulence and Model of Turbulent Transport in the Atmospheric Surface Layer. SRC RAS, Sochi,. 160 p. (in Russian)
56. Trunev, A.P. 3D Turbulent Boundary Layer Model Based on Organized Motion Theory/ In The Final Proceedings for Organized Vortical Motion as a basis for Boundary-Layer Control, 20-22 September 2000, Kiev. http://www.dtic.mil/cgi-bin/GetTRDoc?AD=ADA389323&Location=U2&doc=GetTRDoc.pdf
57. Watson, M.A.P. 1970 The performance of a square rib type of heat transfer surface. CEGB RD/B/N 1738, Berkeley Nuclear Laboratories.
58. Webb, R. L., Eckert, E.R.G. & Goldstein, R. J. 1971 Heat transfer and friction in tubes with repeated-rib roughness. *Int. J. Heat Mass Transfer*, **14**, 601-617.
59. Wieringa, J. 1992 Updating the Davenport Roughness Clarification. *J. Wind Engineer. Industl. Aerodyn.* **41**, 357–368.